Front. Earth Sci. 2018, 12(1): 215–236
https://doi.org/10.1007/s11707-017-0642-3

RESEARCH ARTICLE

Earthquake hazard potential in the Eastern Anatolian Region of Turkey: seismotectonic *b* and *Dc*-values and precursory quiescence *Z*-value

S. ÖZTÜRK (✉)

Gümüşhane University, Department of Geophysics, TR-29100, Gümüşhane, Turkey

Abstract The Eastern Anatolian Region of Turkey is one of the most seismically and tectonically active regions due to the frequent occurrence of earthquakes. Thus, the main goal of this study is to analyze the regional and temporal characteristics of seismicity in the Eastern Anatolia in terms of the seismotectonic *b*-value, fractal dimension *Dc*-value, precursory seismic quiescence *Z*-value, and their interrelationships. This study also seeks to obtain a reliable empirical relation between *b* and *Dc*-values and to evaluate the temporal changes of these parameters as they relate to the earthquake potential of the region. A more up-to-date relation of $Dc = 2.55 - 0.39*b$ is found with a very strong negative correlation coefficient ($r = -0.95$) by using the orthogonal regression method. The *b*-values less than 1.0 and the *Dc*-values greater than 2.2 are observed in the Northeast Anatolian Fault Zone, Aşkale, Erzurum, Iğdır and Çaldıran Faults, Doğubeyazıt Fault Zone, around the Genç Fault, the western part of the Bitlis-Zagros Thrust Zone, Pülümür and Karakoçan Faults, and the Sancak-Uzunpınar Fault Zone. In addition, the regions having small *b*-values and large *Z*-values are calculated around the Genç, Pülümür and Karakoçan Faults as well as the Sancak-Uzunpınar Fault Zone. Remarkably, the combinations of these seismotectonic parameters could reveal the earthquake hazard potential in the Eastern Anatolian Region of Turkey, thus creating an increased interest in these anomaly regions.

Keywords Eastern Anatolia, *b*-value, fractal dimension, precursory seismic quiescence, earthquake hazard

Received October 12, 2016; accepted January 23, 2017

E-mail: serkanozturk@gumushane.edu.tr

1 Introduction

Numerous statistical studies on the regional and temporal variations of seismicity have been conducted to analyze the characteristics of seismic activity in Turkey as well as various other regions of the world. The use of a variety of tools, such as physical models and scaling laws, have resulted in considerable findings (e.g., Mandelbrot, 1982; Hirata, 1989a; Hirabayashi et al., 1992; Frohlich and Davis, 1993; Matcharashvili et al., 2000; Öncel and Wilson, 2007; Roy et al., 2011; Öztürk, 2011, 2012, 2015). Different seismic parameters can be used in these studies. The following tools can be used as size-scaling parameters: 1) regional, temporal, and magnitude distribution of seismicity, magnitude completeness *Mc*-value, 2) *b*-value, which defines the frequency-magnitude distribution of earthquakes, 3) fractal dimension *Dc*-value, defined as the number of objects greater than a specified size with a power law dependent on size, and 4) standard deviate *Z*-value, one of the best known tools used for the assessment of precursory seismic quiescence before earthquake occurrence in a given region.

Fractal and chaotic properties of earthquakes are recognized and detailed with the application of fractal concepts to seismicity in Goltz (1998). Fractal properties characterize the evolution of earthquake system to a self-organized critical state. It is well known that tectonically and seismically active regions exhibit a fractal correlation or scale invariant between earthquakes both spatially and temporarily (Öncel et al., 1995). One of the best known power-law relations is fractal and it can be given as a two-point regional correlation function for the epicenter of earthquakes (Mandelbrot, 1982). A fractal is an object or set of non-integer dimensions and a fractal dimension is an expression of statistical self-similarity or scale invariance (Goltz, 1998). This is a sophisticated statistical tool in quantifying the earthquake distributions, its randomness, and clustering (e.g., Hirata, 1989a; Ouillon et al; 1995, Teotia and Kumar, 2007). Some structural, geological, or mechanical changes in heterogeneity can be described by using fractal dimension and can also define the heterogeneity of seismicity in an active fault system. As a result, an assessment of the relationship between fractal properties of complex seismotectonic parameters may determine the seismic risk and hazard analyses for a given region. The fractal dimension of earthquakes has recently been used as a powerful tool to quantify the basic properties of a system or a process having fractal properties (e.g., Hirata, 1989b; Öncel et al., 1995; Matcharashvili et al., 2000; Öncel and Wilson, 2002, 2004; Chen et al., 2006; Öztürk, 2012).

The *b*-value, as stated in the Gutenberg-Richter frequency-magnitude relation, is another power-law distribution of earthquakes (Gutenberg and Richter, 1944). A fractal correlation between earthquake frequency and seismic energy, moment, or fault length can be provided by estimating the *b*-value. The *b*-values not only reflect the relative proportion of the small and large earthquakes, but can also be related to the characteristics of the seismogenic structures and the stress changes in space, time, and depth (Mogi, 1967; Mori and Abercrombie, 1997; Wyss et al., 2001). If the *b*-value shows a decreasing trend in a region, a strong or large earthquake is likely to occur (Prasad and Singh, 2015). As such, the *b*-value is one of the best known seismicity parameters which describes the size distribution of earthquakes. Numerous and varied studies for spatial or temporal analyses are conducted across the globe, yet in Turkey the *b*-value is used (e.g., Wiemer and Katsumata, 1999; Enescu and Ito, 2002; Öztürk et al., 2008; Öztürk, 2011, 2015).

In recent years, numerous studies have been made on the spatial and temporal variations of seismic quiescence as an earthquake precursor. Although the anomalies of precursory seismic quiescence are controversial, they may be related to precursors that indicate earthquakes. Precursory seismic quiescence is the inner part of the doughnut pattern proposed by Mogi (1969) on the basis of visual inspection of seismicity maps. Wyss and Martirosyan (1998) defined the seismic quiescence as a significant decrease in mean seismicity rate in comparison with the background seismicity (Wu and Chiao, 2006). According to the results from different studies, a decrease in seismic activity may last between one and several years and must precede or lead up to the main shock time. Precursory quiescence hypothesis is described by Wiemer and Wyss (1994) as: "*A statistically significant decrease of the seismicity rate that occurs in a restricted segment of a seismogenic zone. The rate decrease is terminated by a main shock and the quiescent volume covers all or a major part of the source volume*." Some investigations show that precursory seismic quiescence occurred in and around focal areas several years before main shocks, such as in: Tokachi-Oki (Mogi, 1969); San Andreas (Wyss and Burford, 1987); Kurile (Katsumata and Kasahara, 1999); Colfiorito (Console et al., 2000); Elazığ and Van (Öztürk and Bayrak, 2012). Thus, these precursory seismic quiescence evaluations can give evidence to earthquake forecast research and can also achieve a statistical evaluation for detecting the next quiescence period in real time for a given region.

Given Turkey has been observed as one of the most active earthquake regions in the world, numerous studies on the seismic behaviors of the earthquakes for seismic risk and hazard assessments have been conducted. However, these types of studies, which have a possible correlation between seismic and tectonic parameters, are relatively rare for the Eastern Anatolian Region. The Eastern Anatolian Region is one of the most seismically active, with many destructive earthquakes occurring in recent years, such as in 26 December 1939 Erzincan (*M*8.0), 17 August 1949 Elmalıdere-Bingöl (*M*7.1), 13 March 1992 Erzincan (*M*6.8), 1 May 2003 Bingöl (*M*6.4), 27 January 2003 Tunceli (*M*6.1), 11 August 2004 Elazığ (*M*5.7) and 25 January 2005 Hakkari (*M*5.9). As a result, these types of applications between seismic and tectonic parameters, as stated above in terms of the regional and temporal characteristics of earthquakes, may give new insights into the assessments of earthquake risks and hazards. Due to the occurrences of the recent strong "M_W = 6.0- Elazığ earthquake, 2010 March 08; M_W = 5.5- Erzincan earthquake, 2011 September 22; M_W = 7.2- Lake Van earthquake, 2011 October 23 and M_W = 5.5- Bingöl earthquake, 2015 December 03," a detailed regional and temporal analysis of seismicity should be conducted to investigate the earthquake potential in the Eastern Anatolian Region of Turkey. In the scope of this study, regional, temporal and magnitude distribution of earthquakes are analyzed in terms of size-scaling distributions. For this purpose, a statistical assessment is achieved by using seismic and tectonic parameter *b*-value and fractal dimension *Dc*-value, magnitude completeness *Mc*-value, and standard deviate *Z*-value. In addition, an up-to-date and suitable relation between *Dc* and *b*-values are tried to estimate for the Eastern Anatolia.

2 Earthquake catalog and seismotectonic zonation

The earthquake catalog used in this work was compiled from Öztürk (2009) for the period of 1970 to 2006. Öztürk (2009) used some empirical relationships to prepare a complete and homogeneous database, in addition to an instrumental earthquake catalog for duration magnitude M_D, including 73,530 earthquakes from 1970 to 2006 (all details for the relationships of different magnitude types are also suggested by Bayrak et al., 2009). The Bogazici University, Kandilli Observatory and Research Institute (KOERI) catalog is also used for the time interval between 2006 and 2015. KOERI generally provides the type of M_D for all earthquakes, especially after 2000. However, KOERI has supplied a local magnitude M_L for missing M_D in recent years. When M_D is unknown in the KOERI catalog from 2006 to 2015; unknown M_D calculations are made with M_D-M_L relationships supplied by Öztürk (2009). A total of 62,350 earthquakes have been updated for Turkey between 2006 and 2015. The final result showed 165,880 events occurred in and around Turkey from 1970 to 2015.

KOERI has computed the magnitude of events with M_D (sometimes M_L or different magnitude types) and supplies the real time data with the modern on-line and dial-up seismic stations in Turkey, especially after 2000. KOERI determines the magnitude and location of earthquakes as correctly and rapidly as possible. KOERI has a great number of stations in all regions of Turkey and signals from the stations are sent by phone lines or by radio waves to the KOERI seismological center. Concerning the accuracy of the earthquake catalog used in this work, as stated in Öztürk (2011), errors in the epicenters of the earthquakes since the 1970s, are within 0 – 15 km and the errors in magnitudes within 0.2, while the corresponding errors for the events prior to the 1970s are 0 – 30 km in epicenters and 0.5 in the magnitudes (Bogazici University home page, http://www.koeri.boun.edu.tr/). Thus, the epicenters of earthquakes are not relocated and the locations and magnitudes of events given by KOERI are used.

The selection of the boundaries in the study area is based on Öztürk (2012). Öztürk (2012) divided Turkey into 55 different seismotectonic zones by considering the previous studies by Erdik et al. (1999) and Bayrak et al. (2009). Turkey is divided into 24 different seismic zones by Bayrak et al. (2009) regarding: (i) the different zonation studies mentioned above for seismic hazard modeling in Turkey, (ii) solution of focal mechanism given by TUBITAK Marmara Research Center (Scientific and Technological Research Council of Turkey) for the great earthquakes that occurred in Turkey between 1977 and 2002 and, (iii) plotting the existing tectonic structure with the epicenter distribution of earthquakes. However, 37 source zones are defined by Erdik et al. (1999) by using whole available data and considering the studies and zonations presented by different researchers. Some parts of these seismogenic zones for the Eastern Anatolia are considered for this analysis. Thus, the Eastern Anatolia Region of Turkey, which is limited by the coordinates 36°N and 42°N in latitude and 36°E and 45°E in longitude, is divided into 21 seismotectonic sub-regions.

The earthquake catalog in this area was prepared for a detailed analysis after the selection of the Eastern Anatolia catalog. First, the events that occurred from 1970 to 2015 were selected catalog with an M_D magnitude type. This catalog is complete for all study periods and for all magnitude levels. Second, the earthquake catalog was prepared for the period of 6 January 1970 to 31 December 2014 with a time length of about 44.70 years. A final a total of 33,865 events with magnitudes $\geqslant 1.0$ and a depth of < 70 km in these coordinates from 1970 – 2015 was obtained.

3 Seismotectonic structure in the Eastern Anatolian Region

The East Anatolian Fault Zone (EAFZ) is a transform fault and forms the boundaries between the Arabian and African plates and the Anatolian and the Eurasian plates. This zone measures approximately 550 km in length and is a sinistral strike-slip fault zone that comprises a series of faults arranged parallel, subparallel, or obliquely and is generally northeast-trending. The fault zone is thought to be a conjugate structure to the North Anatolian Fault Zone (NAFZ). The EAFZ starts at Karlıova in the northeast and reaches to Kahramanmaraş in the southwest. It meets and forms triple junctions with the NAFZ and the Dead Sea Fault Zone (DSFZ), respectively (Bozkurt, 2001).

Another structure in this region is the DSFZ and is 1000 km long. This zone is a sinistral intraplate strike-slip fault zone, in an approximate north-south direction. The DSFZ is considered a plate boundary of transform type and separates the Arabian Plate to the east and the African Plate to the west (Şengör and Yılmaz, 1981). The African Plate moves northward slower than the Arabian Plate. The DSFZ takes up this dissimilar motion between the plates. In regard to tectonics, the DSFZ combines the divergent plate boundary along the Red Sea with the plate convergence along the Alpine-Himalayan belt in southern Turkey (Hempton, 1987). Thus, the DSFZ and EAFZ meet in a triple junction between the Anatolian, African, and Arabian Plates near Kahramanmaraş.

The Eurasian and the Arabian Plates collide along the Bitlis-Zagros Thrust Zone (BZTZ) resulting in the uplift of mountains along the suture zone. The BZTZ is a complex collisional boundary of continent-ocean and continent-continent. This boundary reaches to the north of the fold-and-thrust belt of the Arabian platform and extends from southeastern Turkey to the Zagros Mountains in Iran (Şengör and Yılmaz, 1981).

A north-south compressional tectonic regime is dominant in the area east of the Karlıova triple junction. This region is characterized by two strike-slip faults types: sinistral and dextral, running parallel to the North and East Anatolian Fault Zones (Bozkurt, 2001). Compressional basins with east-west trending give shape to the most spectacular structures in the region although the conjugate strike-slip fault system dominates the major tectonics of Eastern Anatolia. Simplified neotectonic structures and provinces modified from Bozkurt (2001) are given in Fig. 1(a). Major tectonic structures in Eastern Anatolia were updated by Şaroğlu et al. (1992) and Bozkurt (2001), and plotted in Fig. 1(b). As seen in Fig. 1(b), there are several major tectonics in the study area, including: Ağrı,

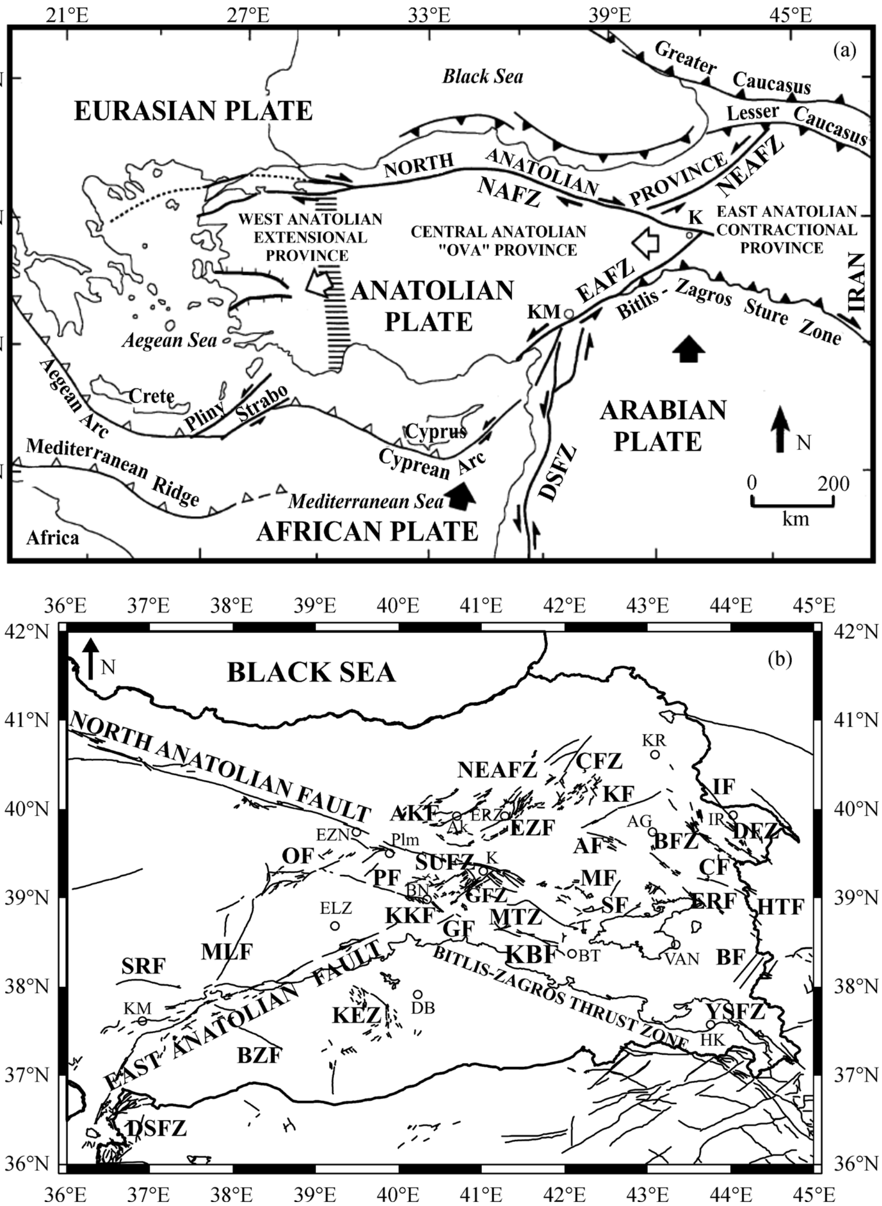

Fig. 1 (a) Simplified tectonic environments in and around Turkey demonstrating main neotectonic structures and provinces (replaced from Bozkurt, 2001). K: Karlıova, KM: Kahramanmaraş. (b) Major tectonic faults in the Eastern Anatolia area of Turkey. Some city locations are shown: AG: Ağrı, Ak: Aşkale, BN: Bingöl, BT: Bitlis, DB: Diyarbakır, ELZ: Elazığ, ERZ: Erzurum, EZN: Erzincan, HK: Hakkari, IR: Iğdır, K: Karlıova, KM: Kahramanmaraş, KR: Kars, Plm: Pülümür. Major structures were taken from Şaroğlu et al., (1992) and Bozkurt (2001). Names of the faults: AF: Ağrı fault, AKF: Aşkale fault, BF: Başkale fault, BFZ: Balıklıgölü Fault Zone, BZF: Bozova fault, ÇF: Çaldıran fault, ÇFZ: Çobandede Fault Zone, DFZ: Doğubeyazıt Fault Zone, DSFZ: Dead Sea Fault Zone, ERF: Erciş fault, EZF: Erzurum fault, GF: Genç fault, GFZ: Göynük Fault Zone, HTF: Hasan-Timur Fault, IF: Iğdır fault, KBF: Kavakbaşı Fault, KEZ: Karacadağ Extension Zone, KF: Kağızman fault, KKF: Karakoçan fault, MLF: Malatya fault, MF: Malazgirt fault, MTZ: Muş Thrust Zone, NEAFZ: North East Anatolian Fault Zone, OF: Ovacık fault, PF: Pülümür fault, SF: Süphan fault, SRF: Sürgü fault, SUFZ: Sancak-Uzunpınar Fault Zone, YŞFZ: Yüksekova-Şemdinli Fault Zone.

Aşkale, Başkale, Bozova, Çaldıran, Erciş, Erzurum, Genç, Hasan-Timur, Iğdır, Kağızman, Karakoçan, Kavakbaşı, Malatya, Malazgirt, Ovacık, Pülümür, Süphan, and Sürgü faults, Balıklıgöl, Çobandede, Doğubeyazıt, Göynük, North East Anatolia, Sancak-Uzunpınar, and Yüksekova-Şemdinli fault zones, Karacadağ Extension, and Muş Thrust zones. Epicenters of these earthquakes, as well as the 21 seismotectonic zones in the Eastern Anatolian Region, for this time interval are shown in Fig. 2.

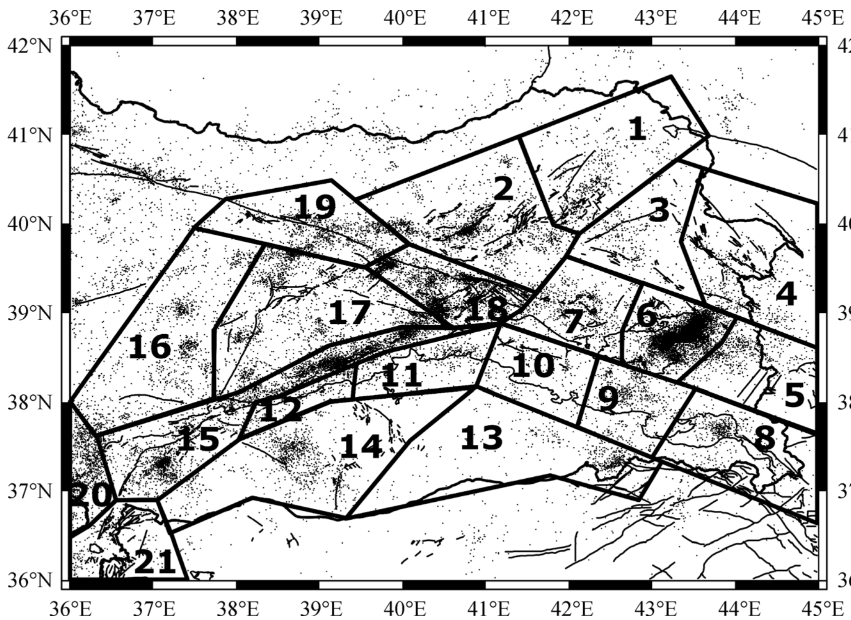

Fig. 2 Seismic and tectonic sub-regions and the epicenters of 33,865 shallow (depth < 70 km) earthquakes with $M_D \geqslant 1.0$ between 1970 and 2015.

4 Methods of analysis and their brief descriptions

In this study, several important seismotectonic parameters, such as the *b*-value of magnitude-frequency distribution of earthquakes, *Dc*-value of fractal dimension of earthquake occurrences, and *Z*-value of precursory seismic quiescence, are discussed in terms of variations in space and time of seismicity in the Eastern Anatolian Region of Turkey.

4.1 Gutenberg-Richter (G-R) relation (*b*-value) and completeness magnitude (*Mc*-value)

Gutenberg-Richter (1944) described the relation between magnitude and frequency of occurrence of earthquakes as a power-law of size distribution of earthquakes. It can be given as:

$$\log_{10} N(M) = a - bM, \tag{1}$$

where *N*(*M*) is the expected number of earthquakes with magnitudes equal to or larger than *M*, *b*-value defines the slope of the magnitude-frequency distribution, and *a*-value is related to the seismic activity rate. The *a*-value shows different values for different regions. These changes depend on the length of the study area, observation period, and number of earthquakes. The *b*-value for different regions may change roughly from 0.3 to 2.0 and is a measure of the proportion of larger to smaller events within a set of earthquakes. However, Frohlich and Davis (1993) stated that the regional scale estimates of the average *b*-value are approximately equal to 1. The variations in *b*-value can be a result from many factors, such as the geological complexity and degree of heterogeneity of cracked medium, strain, and stress conditions in the region. Many factors can also cause variations in *b*-value: (i) *b*-value decreases before a large earthquake, (ii) increases prior to, and then decreases sharply, immediately before a large earthquake, (iii) changes throughout an aftershock sequence, and (iv) exhibits variation over large areas and longtime intervals, not apparently related to large events (e.g., Mogi, 1967; Wyss et al., 2001).

It is well known in the seismicity studies that magnitude completeness, *Mc*-value, has been used as a significant parameter, especially in the calculation of *b*-value in G-R relationship. Using the maximum number of events is necessary for high quality and suitable outputs. *Mc*-value can be estimated by the assumption of G-R distribution versus magnitude. A moving time window approach is used to calculate the variation in *Mc*-value (Wiemer and Wyss, 2000). Temporal variations of *Mc*-value can cause wrong analyses in the estimation of seismicity parameters, especially in *b*-value, if the magnitude completeness shows systematically significant fluctuations as a function of time and space. As a result, this type of completeness analysis for the catalog used in this study is a significant process because a part of this study uses *Mc*-value in the calculation of *b*-value and *Z*-value.

4.2 Fractal dimension (*Dc*-value)

Earthquake distributions are considered fractal and fractal dimension is a real number which measures the geometry of a distribution and presumably varies as a function of time and space. Fractal analysis is often used to evaluate the clustering properties and size scaling attributes of seismotectonic parameters. Using the two-point correlation dimension *Dc*, it is demonstrated that spatial and temporal patterns of earthquake occurrence is fractal. *Dc* analysis is a significant tool for quantifying the self-similarity of a geometrical object. A further generalization leads to the correlation dimension *Dc* which is not based on a covering of the regarded set, but on the distances between pairs of points of the set (Goltz, 1998). An algorithm based on distances between pairs of points, called sphere counting, was introduced by Grassberger and Procaccia (1983). This correlation dimension is among the most widely used. Grassberger and Procaccia (1983) described the correlation dimension *Dc* and the correlation sum *C*(*r*) as:

$$Dc = \lim_{r \to 0}[\log C(r)/\log r], \quad (2)$$

and

$$C(r) = 2N_{R<r}/N(N-1), \quad (3)$$

where *C*(*r*) is the correlation function, *r* is the distance between two epicenters and *N* is the number of event pairs separated by a distance $R < r$. If the epicenter distribution has a fractal structure, the following relation is given:

$$C(r) \sim r^{Dc}, \quad (4)$$

where *Dc* is a fractal dimension; more generally, the correlation dimension. The distance *r* (in degrees) between two earthquakes can be computed from:

$$r = \cos^{-1}\left(\cos\theta_i\cos\theta_j + \sin\theta_i\sin\theta_j\cos(\phi_i - \phi_j)\right), \quad (5)$$

where (θ_i, ϕ_i) and (θ_j, ϕ_j) are the latitudes and longitudes of the i^{th} and j^{th} earthquakes, respectively (Hirata, 1989a). Fractal dimension *Dc* is estimated from the slope of the plotting graph *C*(*r*) against *r* on a double logarithmic coordinate. The extremes of the finite range of scales generate undesirable edge effects. When *r* is small, *C*(*r*) is unaffected by the lack of points outside the cluster. Hence, *C*(*r*) increases rapidly with *r*, and *Dc* is large. Therefore, if a scaling range using small values of *r* is used to calculate *Dc*, strong clustering would correspond to an increase in *Dc*. When *r* approaches the diameter of the cluster, the rate at which *C*(*r*) increases with *r* decreases, and *Dc* will be small. Hence, if a scaling range using large values of *r* is used to calculate *Dc*, strong clustering would correspond to a decrease in *r*. This implies that, depending on the range of *r* chosen, a dense cluster of points can yield both high and low values of *Dc*. In practice, fractal systems in nature are self-similar over a finite range, so *Dc* must be estimated from a range insensitive to the finiteness of the set.

Fractal distributions imply that the number of objects larger than a specified size has a power law dependent on the size. Fractal distributions are also the only distributions that do not include a characteristic length scale, and therefore, are applicable to scale invariant phenomena. As earthquake distributions obey fractal statistics, fractal dimension can characterize them. Thus, the nature of spatial and temporal characteristics of the earthquakes is defined by correlation dimension. This parameter can be estimated in order to find the possible unbroken sites which have been mentioned as seismic gaps that may be broken in the future (Kagan, 2007). That means that the variations in fractal features depend on the complexity or quantitative measure of the heterogeneity degree of seismic activity on the fault systems. Higher *Dc*-value associated with lower *b*-value is the dominant structural property in areas of increased complexity of the active fault system and may be a caused by the clusters. As a result, fluctuations in this parameter may be an indication of stress changes on the fault planes of smaller surface areas (Öncel and Wilson, 2002; Polat et al., 2008).

4.3 Method to decluster the earthquake catalog and a description of the seismic quiescence method (*Z*-value)

The algorithm of cluster analysis "declusters" or decomposes an earthquake catalog into main and secondary events (Arabasz and Hill, 1996). All dependent events from each cluster can be removed with this process and they can be substituted with a unique event. Extracting the dependent events from the catalog is an important part of a quantitative seismic quiescence analysis. In this study, the Reasenberg (1985) algorithm is used to decluster the earthquake catalog and separate the dependent from the independent events. *ZMAP* software, introduced by Wiemer (2001), is used for the declustering method based on the algorithm developed by Reasenberg (1985). After Wiemer (2001), many studies were conducted on the seismic quiescence by using *ZMAP* software (e.g., Wyss et al., 2004; Polat et al; 2008; Öztürk, 2011, 2013, 2015; Öztürk and Bayrak, 2012).

In this study, the earthquake catalog is declustered with the Reasenberg (1985) algorithm and is then used for detecting the seismic quiescence areas. It has documented 33,865 earthquakes with magnitudes$\geqslant$1.0 between 1970 and 2015. For whole catalogs from 1970 to 2015, the average *Mc*-value was estimated at 2.9 and the number of earthquakes with a magnitude of $M_D < 2.9$ were found as 19,310. All events with magnitude $M_D < 2.9$ are subtracted from the catalog and thus, the number of events exceeding this magnitude threshold is found as 14,555. Using the declustering algorithm, 4087 (about 28%) earthquakes are subtracted and about 69% of all earthquakes in total were removed from the catalog. As a result, the number of events for seismic quiescence analysis in the Eastern Anatolia was reduced to 10,468. This declustered catalog is accepted as the final version.

Numerous techniques have been used to identify and describe seismicity rate changes, many of which use seismic quiescence phenomenon. The best known for seismic quiescence analysis is the standard normal deviate *Z*-test. The *ZMAP* technique is used to find regions showing seismic quiescence (for details see Wiemer and Wyss, 1994). This algorithm generates the Log Term Average, LTA(*t*), function for the statistical evaluation of the confidence level in units of standard deviations:

$$Z(t) = \frac{R_{all} - R_{wl}}{\sqrt{\frac{\sigma_{all}^2}{n_{all}} + \frac{\sigma_{wl}^2}{n_{wl}}}},$$

where R_{wl} is the mean seismicity rate in the foreground window, R_{all} is the average number of earthquakes for the entire background period, and σ and n are the standard deviations and the number of samples, within and outside the window. The *Z*-value computed as a function of time, letting the foreground window slide along the time duration of catalog, is called LTA (*t*).

5 Results of analyses and discussion

The main goal of this study is to investigate the correlations between various seismotectonic parameters, such as Gutenberg-Richter *b*-value, fractal correlation dimension *Dc*-value, and seismicity rate changes *Z*-value in the Eastern Anatolian Region. An analyses is performed by plotting the histograms of the spatial, temporal, and magnitude distribution during the time period of 1970 to 2015. It is well known that the earthquake seismicity and fractal properties relationship characterizes the complex properties and patterns of the earthquake seismicity. Thus, a reliable statistical relationship between the seismotectonic *b*-value and correlation dimension *Dc*-value is used to estimate the potential for earthquakes in the Eastern Anatolian Region. The study region is divided into 21 seismotectonic sub-regions to perform a detailed statistical analysis between *b* and *Dc*-values, accomplished by employing *ZMAP* software. The maximum likelihood estimation is used to estimate the *b*-values, because it yields a more robust estimate than the least-square regression method (Aki, 1965). The *Dc*-values in all sub-regions are found with 95% confidence limits by linear regression.

The completeness magnitude *Mc* is one of the most significant statistical parameters for many seismicity studies and typically has a non-stable value in space and time. It is a fact that the usage of the maximum number of earthquakes for high quality results has a great importance in seismicity analyses. The variations in *Mc*-value as a function of time is made by using a moving window approach with maximum curvature method (Woessner and Wiemer, 2005). In order to estimate the *Mc*-value, the earthquake catalog, including all 33,865 earthquakes with $M_D \geqslant 1.0$, is used and *Mc* is drawn with its standard deviation for samples of 50 events/windows. Variation in *Mc*-value with time is plotted in Fig. 3. *Mc*-value is quite large until 1995 when it changes to between 4.0 and 4.6. However, it varies from approximately 4.0 to 3.0 between 1995 and 2000 followed by an observed change between 2.5 and 3.5 from 2000 to 2010. Between 2005 and 2010, the *Mc*-value is approximately 3, followed by a variance between 3.0 and 2.0 after 2010. Because this study focuses on the magnitude-frequency distribution of the earthquakes and the seismic quiescence analysis, *Mc* is of significant importance. Consequently, *Mc*-value for this region of Turkey changes between 2.4 and 3.0, which is in accordance with the results of Öztürk and Bayrak (2012).

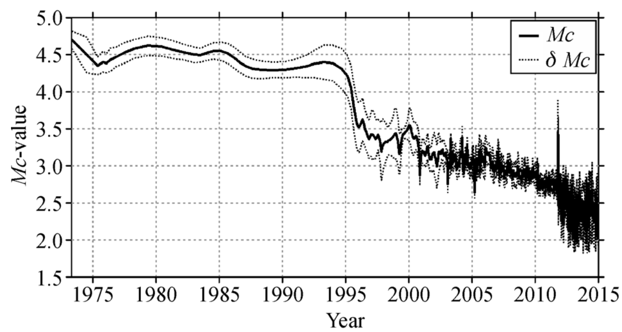

Fig. 3 Changes in magnitude completeness, *Mc*-value, from 1970 to 2015 in the Eastern Anatolian region of Turkey. Standard deviation (*δMc*) of the completeness is plotted with dashed line. Completeness is illustrated with overlapping samples and each sample contains 50 events.

Figure 4 shows the cumulative number of earthquakes against time for the original catalog, including all dependent 33,865 events with $M_D \geqslant 1.0$ and for the declustered catalog, including 10,468 independent events obtained from the original catalog including 14,555 earthquakes with $M_D \geqslant 2.9$ between 1970 and 2015. As seen in Fig. 4, no significant seismic activity is observed

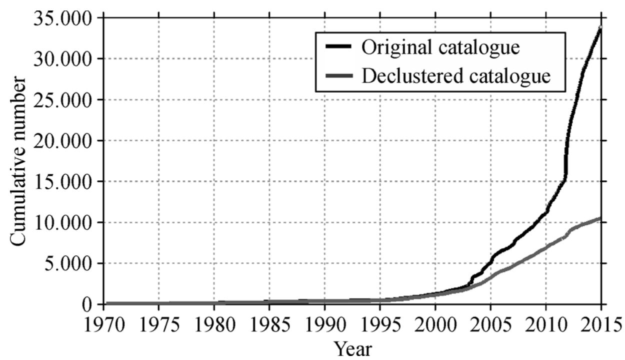

Fig. 4 Cumulative number of events as a function of time for the original catalog, including all earthquakes with $M_D \geqslant 1.0$, and for the declustered catalog, including the events of $M_D \geqslant 2.9$ in the Eastern Anatolian Region of Turkey.

from 1970 to 1995, and there is a little variation between 1995 and 2000. Conversely, there is an important seismic activity after 2000. The cumulative number of declustered events with $M_D \geqslant 2.9$ as a function of time for the region has a smoother slope than that of the original catalog. It can be easily seen from Fig. 4 that Reasenberg's declustering method has removed dependent events from the original catalog. As a result, the declustering algorithm provided a more homogeneous, reliable, and robust earthquake catalog.

The two estimated parameters with standard deviations as well as tectonic environments, the number of earthquakes, and the completeness magnitudes for all seismotectonic zones considered in this study are shown in Table 1. Also, the figures showing the *Mc*-value, *b*-value, and *Dc*-value estimations for each sub-region are plotted in Fig. 5 and Fig. 6, respectively. As seen in Table 1 and Fig. 5, the *b*-value varies from 0.66 to 1.60. The *b*-values smaller than 1.0 are estimated in regions 1, 4, 5, 9, 11, 12, 18, and 20, including NEAFZ, ÇFZ, IF, ÇF, DFZ, BF, HTF, KBF, some areas of the BZTZ, KKF, SUFZ, GFZ, and the southwest of the EAFZ. Moderate values between 1.0 and 1.1 are calculated in regions 3, 6, 13, 15, 19, and 21, covering AF, KF, BFZ, ERF, SF, the southern area of the BZTZ, EAFZ, eastern area of the NAFZ, and the northern area of the DSFZ. The largest *b*-value is calculated as 1.60 in region 14, including KEZ and BZF. The *b*-values changing between 1.1 and 1.2 are estimated in sub-regions 2, 7, 8, 10, 16 and 17 consisting of AKF, EZF, MF, MTZ, YŞFZ, GF, SRF, PF, MLF, and OF. The spatial variation of *b*-value is also mapped by considering the spatial grid of points with a 0.05° grid, as shown in Fig. 7. The geographical distribution of *b*-value is plotted with a moving window approach by the samples of 300 events/windows and the declustered earthquake catalog, where $M_D \geqslant 2.9$ was used for this estimation. Average *b*-value is approximately equal to 1.0 as stated in Frohlich and Davis (1993). The regions with greater *b*-values have a higher frequency of low-magnitude earthquakes, whereas the regions with small *b*-values are characterized by a high frequency of large-magnitude earthquakes. Some areas of the study region have relatively large *b*-values, which could be interpreted as stress is more easily reduced with a high frequency of small earthquakes. In this situation, it could be explained by large heterogeneity (Polat et al., 2008) and low stress distribution due to high heat flow. It is well known that lower *b*-values indicate the higher stress release. Thus, a low *b*-value in regions 1, 4, 11, and 12 may be an indication of a low degree of heterogeneity, high-strain due to the active tectonics and stress to build up over time, and to be released by events that are less frequent, but large in magnitude (Öncel and Wilson, 2002). As stated in Prasad and Singh (2015), low *b*-values for a given region may indicate the likelihood for the next possible earthquake which thus could be used to forecast major earthquakes. However, in the regions where *b*-values are large, this could be an indication of low stress release by a large number of small earthquakes, and thus, geological complexity is very high. As a general conclusion, calculated *b*-values through the maximum likelihood approach from the G-R method show a good correlation to the tectonics and seismic activity. It follows then that special emphasis must be given to these regions where *b*-values are low.

Table 1 and Figure 6 also show the estimated *Dc*-values, changing from 1.94 to 2.37, for all 21 seismotectonic zones in Eastern Anatolia. *Dc*-values $\leqslant 2.1$ are found in regions 7, 8, and 14, covering MF, MTZ, YŞFZ, KEZ, and BZF. *Dc*-values changing between 2.1 and 2.2 are found in regions 2, 3, 5, 6, 9, 10, 13, 15, 16, 17, 19, 20, and 21 including EZF, AKF, ÇFZ, AF, KF, BFZ, HTF, BF, ERF, SF, KBF, GF, KEZ, EAFZ, SRF, PF, MLF, OF, the eastern area of the NAFZ, the southwest area of the EAFZ, and the northern area of the DSFZ. The *Dc*-values are $\geqslant 2.2$ in the other sub-regions consisting of 1, 4, 11, 12 and 18. These zones cover the NEAFZ, ÇFZ, IF, ÇF DFZ, and some sections of the BZTZ, KKF, GFZ, and SUFZ. As seen in Table 1, *Dc*-values in this region are generally greater than 2.1. The geographical distribution of *Dc*-value is also given in Fig. 8 and plotted with a cell spacing of 0.05° in latitude and longitude. As in the *b*-value spatial map, the declustered catalog with $M_D \geqslant 2.9$ is also used in this calculation. Regions with complex fault patterns show higher *Dc* and lower *b*-values; thus the stress relaxation occurs on fault planes of smaller surface scale (Öncel and Wilson, 2002). Barton et al. (1999) stated that the faults where earthquakes are caused by failure of isolated, small asperities and occurred in clusters are related to the higher *b*-value and lower *Dc*-value. High permeability and a supply of pore fluids resulted in reduced effective stress in these faults. Öztürk (2011) stated that the higher order fractal dimension (specifically > 2.2) in the North Anatolia Fault Zone is increasingly sensitive to heterogeneity in the distribution of magnitudes. However, Öztürk (2015) used this limit value as $Dc = 2.3$ for the Western Anatolian region. As seen in Table 1, average *Dc*-value is around 2.15 for the eastern region of Turkey. However, a few *b*-values (for example, in regions 13 and 15) are > 1.0 in some sub-regions which have *Dc*-values greater than 2.15. For this reason, *Dc*-value of 2.2 is selected as average or a threshold value for discussions. This value suggests that seismicity is more clustered at larger scales (or in smaller areas) in these regions. However, there are seven areas with *b*-values < 1.0 in addition to observed *Dc*-values > 2.2 in a few of these areas. These zones include NEAFZ and ÇFZ (region 1), IF, ÇF, and DFZ (region 4), some sections of BZTZ (regions 11 and 12), and KKF, GFZ, and SUFZ (region 18). The higher *Dc* values ($\geqslant 2.2$) and lower *b*-values (< 1.0) may be the dominant structural properties in these regions and may arise due to clusters since the uniform distribution of events decreases with an increase in the clustering of events. It can also be an indication of

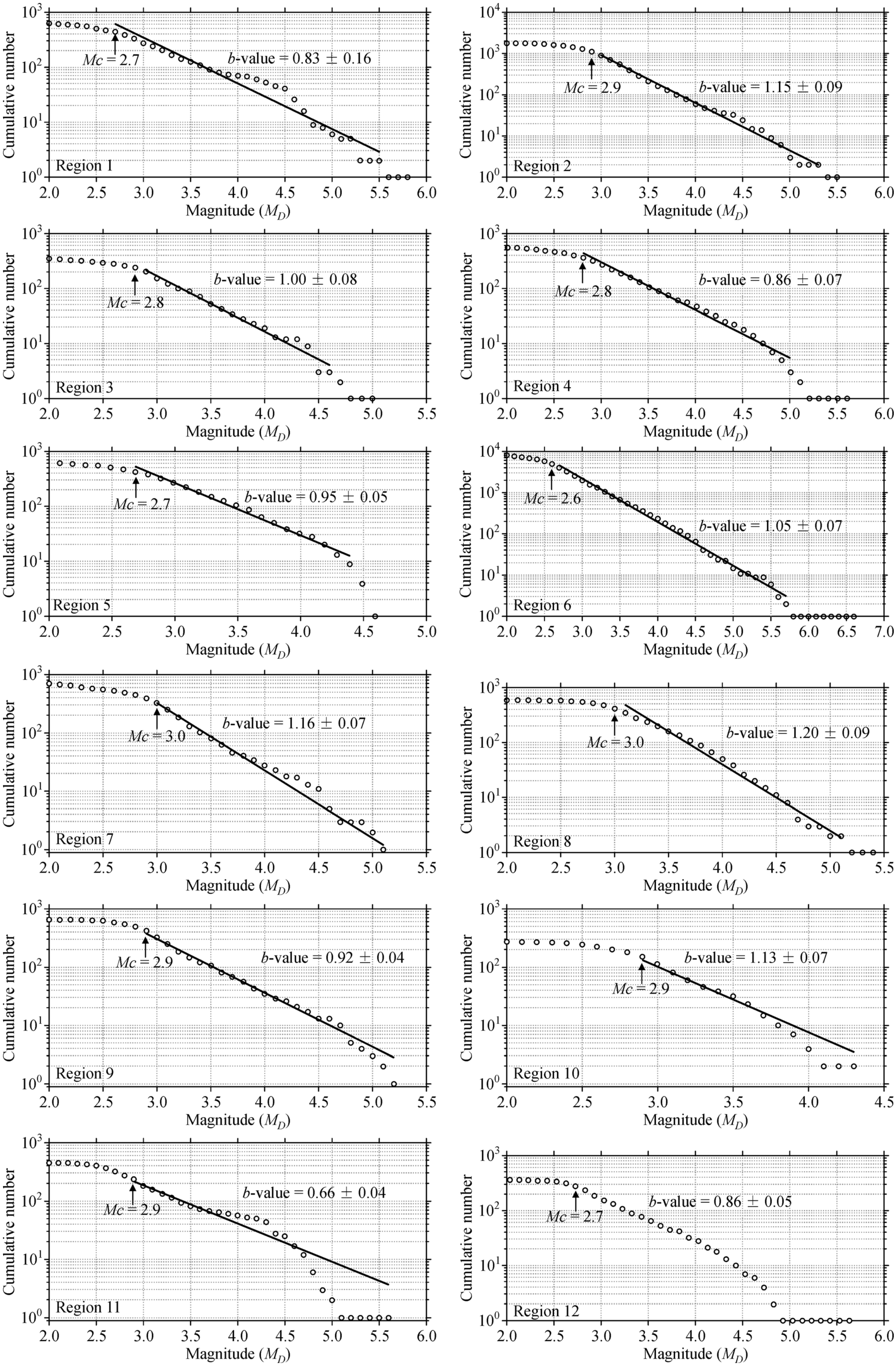
Cumulative number
Magnitude (M_D)
Region 1
Mc = 2.7
b-value = 0.83 ± 0.16
Region 2
Mc = 2.9
b-value = 1.15 ± 0.09
Region 3
Mc = 2.8
b-value = 1.00 ± 0.08
Region 4
Mc = 2.8
b-value = 0.86 ± 0.07
Region 5
Mc = 2.7
b-value = 0.95 ± 0.05
Region 6
Mc = 2.6
b-value = 1.05 ± 0.07
Region 7
Mc = 3.0
b-value = 1.16 ± 0.07
Region 8
Mc = 3.0
b-value = 1.20 ± 0.09
Region 9
Mc = 2.9
b-value = 0.92 ± 0.04
Region 10
Mc = 2.9
b-value = 1.13 ± 0.07
Region 11
Mc = 2.9
b-value = 0.66 ± 0.04
Region 12
Mc = 2.7
b-value = 0.86 ± 0.05

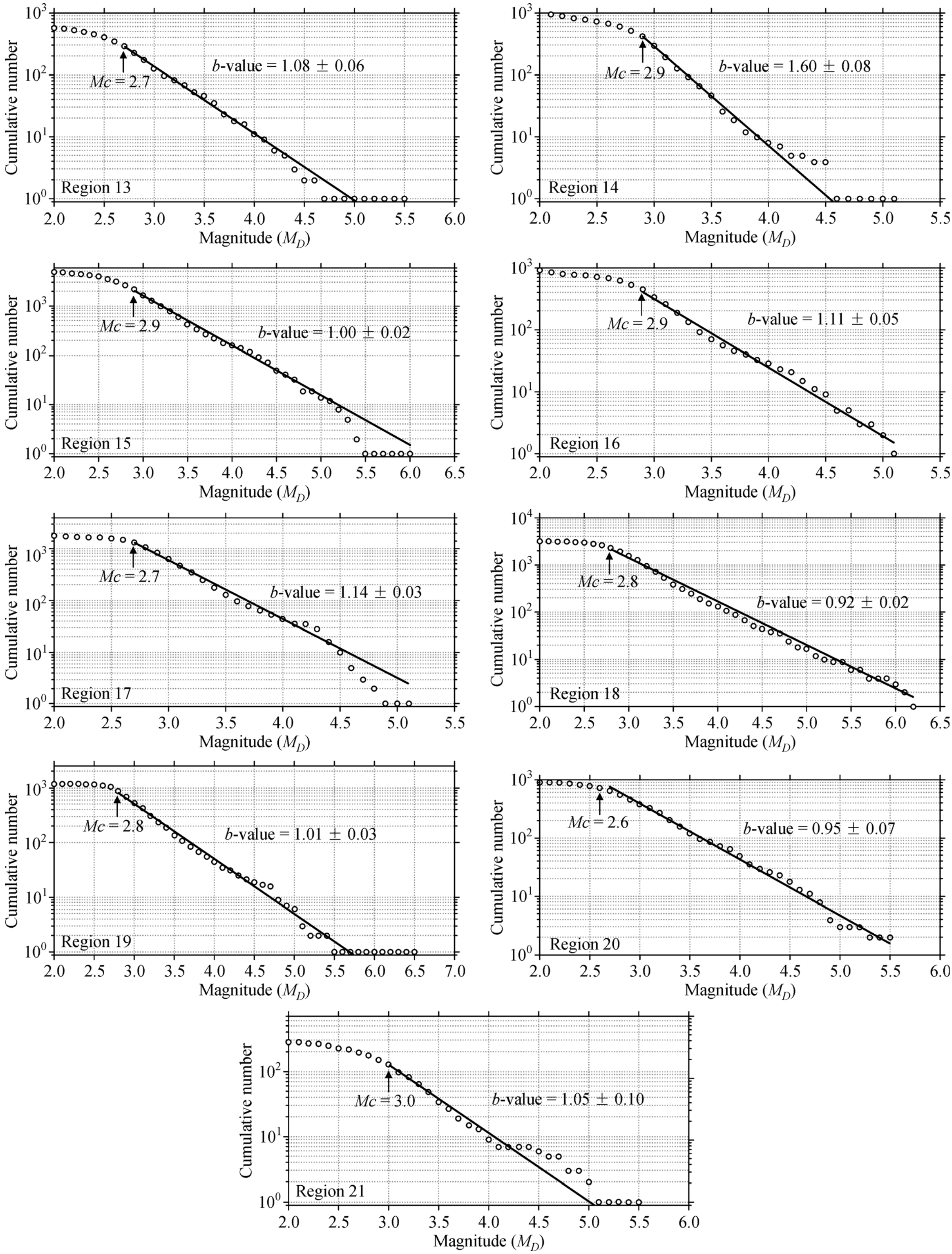

Fig. 5 Gutenberg-Richter relationships and b-values. b-values and their standard deviations as well as the Mc-values are given.

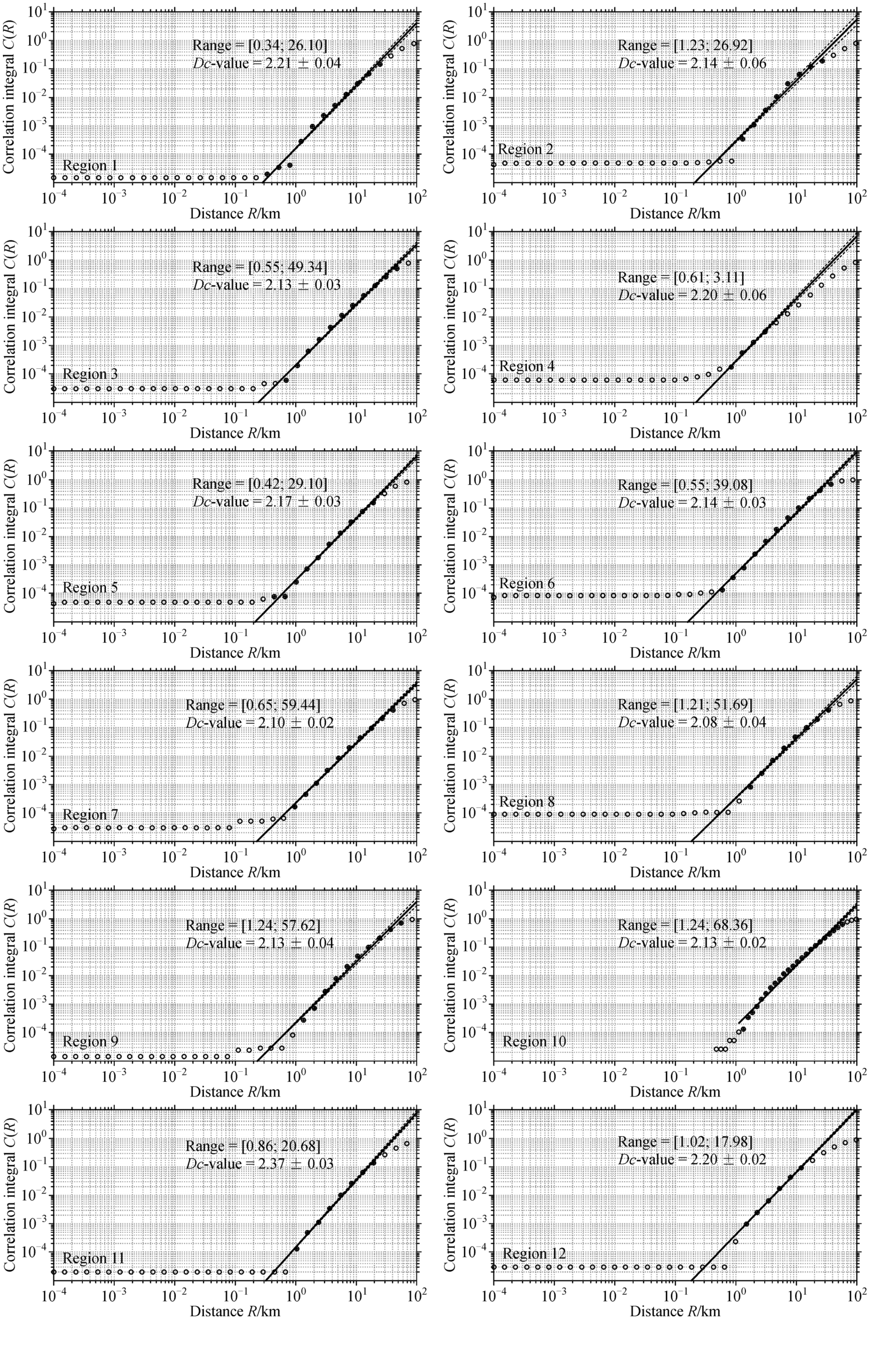
Correlation integral C(R)
Distance R/km
Range = [0.34; 26.10]
Dc-value = 2.21 ± 0.04
Region 1
Range = [1.23; 26.92]
Dc-value = 2.14 ± 0.06
Region 2
Range = [0.55; 49.34]
Dc-value = 2.13 ± 0.03
Region 3
Range = [0.61; 3.11]
Dc-value = 2.20 ± 0.06
Region 4
Range = [0.42; 29.10]
Dc-value = 2.17 ± 0.03
Region 5
Range = [0.55; 39.08]
Dc-value = 2.14 ± 0.03
Region 6
Range = [0.65; 59.44]
Dc-value = 2.10 ± 0.02
Region 7
Range = [1.21; 51.69]
Dc-value = 2.08 ± 0.04
Region 8
Range = [1.24; 57.62]
Dc-value = 2.13 ± 0.04
Region 9
Range = [1.24; 68.36]
Dc-value = 2.13 ± 0.02
Region 10
Range = [0.86; 20.68]
Dc-value = 2.37 ± 0.03
Region 11
Range = [1.02; 17.98]
Dc-value = 2.20 ± 0.02
Region 12

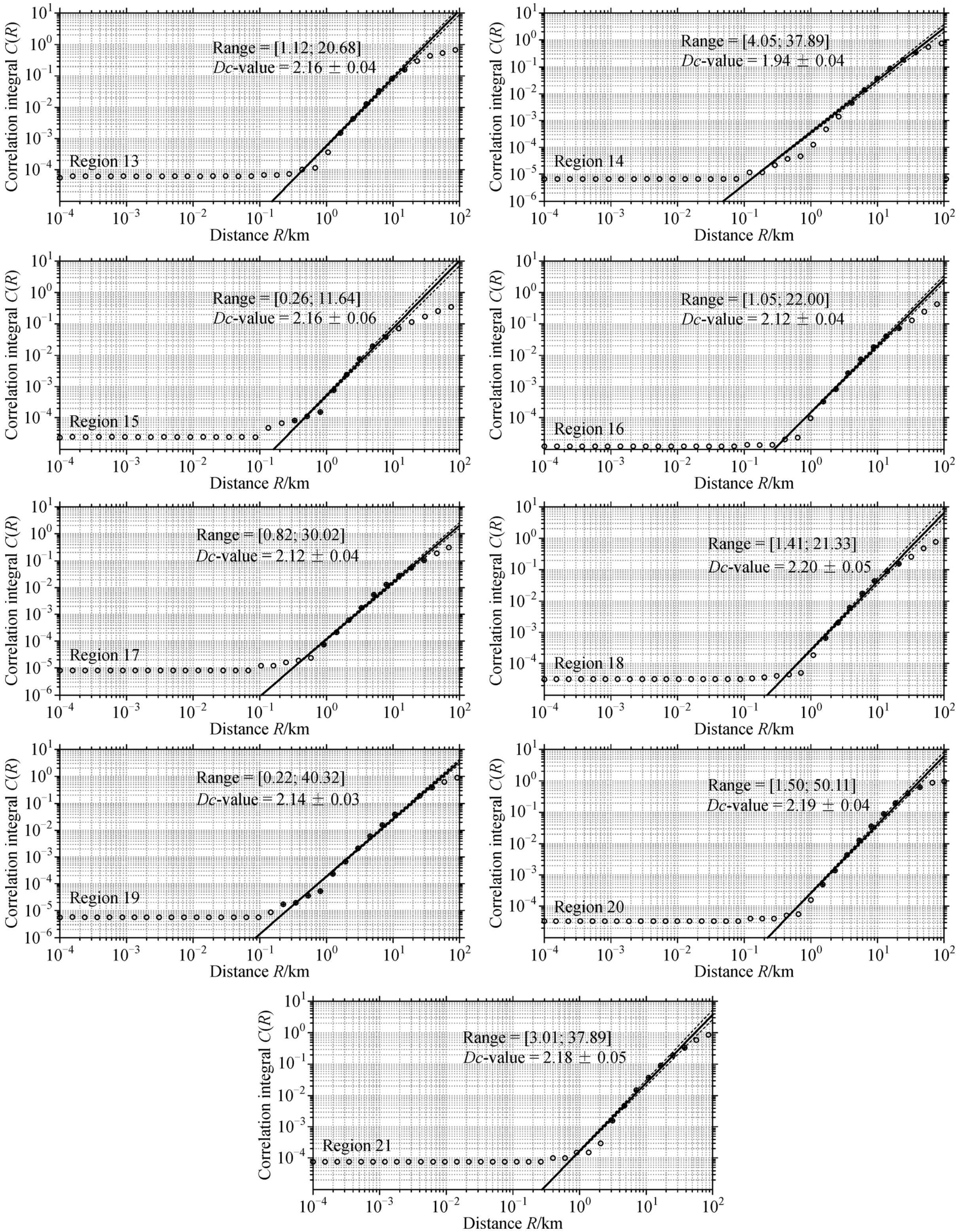

Fig. 6 Correlation integrals and *Dc*-values for all sub-regions. The slope of the black lines corresponds to *Dc*-values and dashed lines illustrate the standard errors.

Table 1 Tectonic structures, earthquake numbers, *Mc*-values, *b*-values and *Dc*-values for different seismic source zones in the Eastern Anatolian Region of Turkey

Region	Tectonic Structures	Earthquake Numbers	*Mc* value	*b*-value	*Dc*-value
1	North East Anatolian Fault Zone, Çobandede Fault Zones	632	2.7	0.83±0.16	2.21±0.04
2	Erzurum Fault, Aşkale Fault	1810	2.9	1.15±0.09	2.14±0.06
3	Ağrı and Kağızman Faults, Balıklıgöl Fault Zone	363	2.8	1.00±0.08	2.13±0.03
4	Iğdır and Çaldıran Faults, Doğubeyazıt Fault Zone	593	2.8	0.86±0.07	2.20±0.06
5	Hasan Timur Fault,	636	2.7	0.95±0.05	2.17±0.03
6	Başkale, Erciş and Süphan Faults	8847	2.6	1.05±0.07	2.14±0.03
7	Malazgirt Fault, Muş Thrust Zone	805	3.0	1.16±0.07	2.10±0.02
8	Yüksekova-Şemdinli Fault Zone,	581	3.0	1.20±0.09	2.08±0.04
9	Kavakbaşı Fault,	649	2.9	0.92±0.04	2.13±0.04
10	Genç Fault,	273	2.9	1.13±0.07	2.13±0.02
11	Some sections of the Bitlis-Zagros	452	2.9	0.66±0.04	2.37±0.03
12	Thrust Zone	361	2.7	0.86±0.05	2.20±0.02
13	Karacadağ Extension Zone,	578	2.7	1.08±0.06	2.16±0.04
14	Bozova Fault	1094	2.9	1.60±0.08	1.94±0.04
15	East Anatolian Fault Zone	5015	2.9	1.00±0.02	2.16±0.06
16	Sürgü Fault	1307	2.9	1.11±0.05	2.12±0.04
17	Pülümür, Malatya and Ovacık Faults	2177	2.7	1.14±0.03	2.12±0.04
18	Karakoçan fault, Göynük and Sancak- Uzunpınar Fault Zones	3187	2.8	0.92±0.02	2.20±0.05
19	Eastern part of the North Anatolian Fault Zone	1180	2.8	1.01±0.03	2.14±0.03
20	Southwest of the East Anatolian Fault Zone	936	2.6	0.95±0.07	2.19±0.04
21	North part of the Dead Sea Fault Zone	283	3.0	1.05±0.10	2.18±0.05

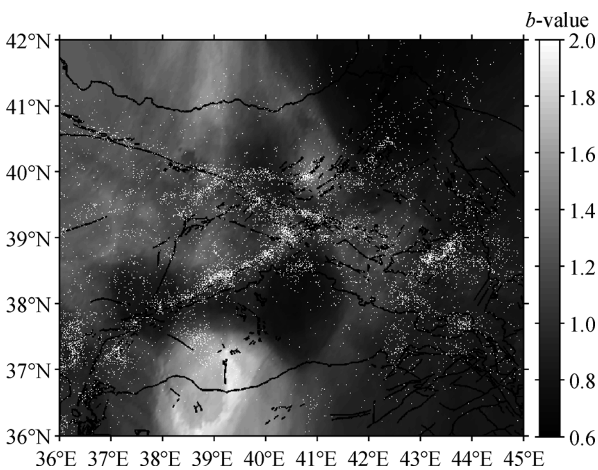

Fig. 7 Regional distribution of *b*-value for the Eastern Anatolian Region of Turkey. The declustered events with $M_D \geqslant 2.9$ are plotted in white dots.

relatively high stress intensity and stronger clustering of epicenters in these regions.

As mentioned above, one of the primary goals of this study is to estimate a reliable statistical relationship between two seismotectonic parameters *b* and *Dc*-values for the Eastern Anatolian earthquakes. For this purpose, the orthogonal regression method (Carrol and Ruppert, 1996) is used to determine the most suitable correlation since the standard least square method is based on the assumption that horizontal axis values are estimated without error. The relationship of orthogonal regression fit between *b* and *Dc*-values is shown in Fig. 9. Also, *Dc*-value against *b*-value for orthogonal regression with fit curve, the corresponding equation, and 95% confidence interval are given in Fig. 9. Also shown in Fig. 9, a very strong negative correlation coefficient ($r = 0.95$) is calculated and the number of events in this confidence limit is 10. Linear regression fit is used and the following relationship is obtained:

$$Dc = 2.55 - 0.39*b, (r = -0.95). \tag{6}$$

A large number of studies on the correlation between *b* and *Dc*-values can be found for different areas of the world (e.g., Aki, 1981; Hirata, 1989a; Roy et al., 2011) and the

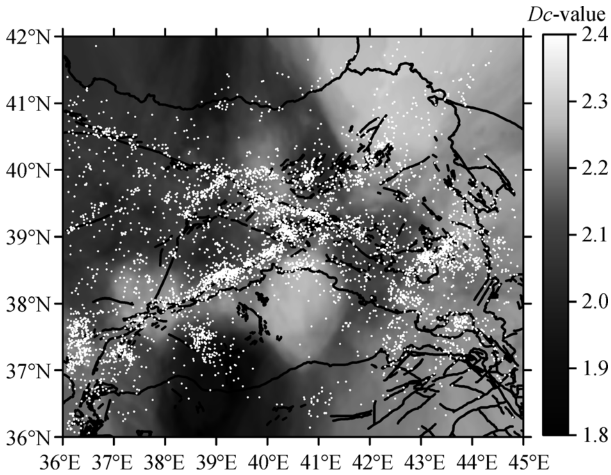

Fig. 8 Regional distribution of *Dc*-value for the Eastern Anatolian Region of Turkey. The declustered events with $M_D \geqslant 2.9$ are marked in white dots.

region of Turkey (e.g., Öncel et al., 1995, 1996; Öncel and Wilson, 2002, 2007; Öztürk, 2011, 2012, 2015). Since Aki (1981) suggested a relationship between *b* and *Dc*-values with a positive correlation $D = 3b/c$ (where *c* is a constant determined from the slope of the log moment against the magnitude relation, *c* is normally taken as 1.5), both the negative (e.g., Hirata, 1989a; Öncel et al., 1995, 1996) and the positive (e.g., Öncel and Wilson, 2004; Roy et al., 2011) correlations between these parameters have been reported for Turkey and different areas of the world.

Aki's fractal dimension may be compared with the correlation dimension, obtained from the spatial distribution of earthquakes. Hirata's (1989a) result does not support Aki's speculation that $D = 3b/c$. On the contrary, there is a negative correlation as $Dc = 2.3 - 0.73*b$ (with $r = - 0.77$) between *b* and fractal dimension of epicenters in the Tohoku Region of Japan. Similarly, a study of seismicity in the North Anatolian Fault Zone of Turkey revealed a long-term negative correlation between *b* and *Dc* (Öncel et al., 1995). The *b*-value was found to be weakly, negatively correlated with fractal dimension as $Dc = 2.74 - 1.52*b$ (with $r = - 0.56$) for the NAFZ in Öncel et al. (1995). Öncel et al. (1996) also investigated the nature of temporal variations in the statistical properties of seismicity associated with the NAFZ between longitudes 31° – 41°E and observed a strong negative correlation ($r = - 0.85$) as $Dc = 2.32 - 1.09*b$. On the contrary, Öncel and Wilson (2002) found a weak positive correlation ($r = 0.48$) between variations in *b* and *Dc* in the western NAFZ. Analysis presented in Öncel and Wilson (2004) reveals a strong positive correlation ($r = 0.81$) along the NAFZ during the time period of 1981 to 1998 preceding the 1999 Izmit earthquake. Öncel and Wilson (2007) observed a strong positive correlation between *Dc* and *b*-values from 1992 – 1994.4 ($r = 0.84$) and 1996.6 – 1998.2 ($r = 0.94$). A negative correlation ($r = - 0.71$) extending from approximately mid-1994 to mid-1996 was observed in northwestern Turkey between 40.5° to 41° north latitude and 29° and 31° east longitude. As a result, estimated relation, correlation coefficient, and the number of events in the confidence limit obtained from orthogonal regression supplies a reliable assessment for the seismotectonics of the Eastern Anatolian earthquakes.

Estimated *b* and *Dc*-values, as well as the number of earthquakes, minimum ($M_{\min}$) and maximum ($M_{\max}$) magnitudes, *M*c-values, and *a*-values, observed annually from 1970 – 1996, are given in Table 2. To evaluate the seismic activity in time, the temporal distribution of all $M_D \geqslant 1.0$ earthquakes from 1970 to 2015 is illustrated in Fig. 10. As seen in Table 2, there were four strong events > 5.5 between 1970 and 1996, with many strong events recorded after 1996. Magnitude-time analysis shows an increase in the number of strong earthquakes after 2000. Major earthquake events, characterized by

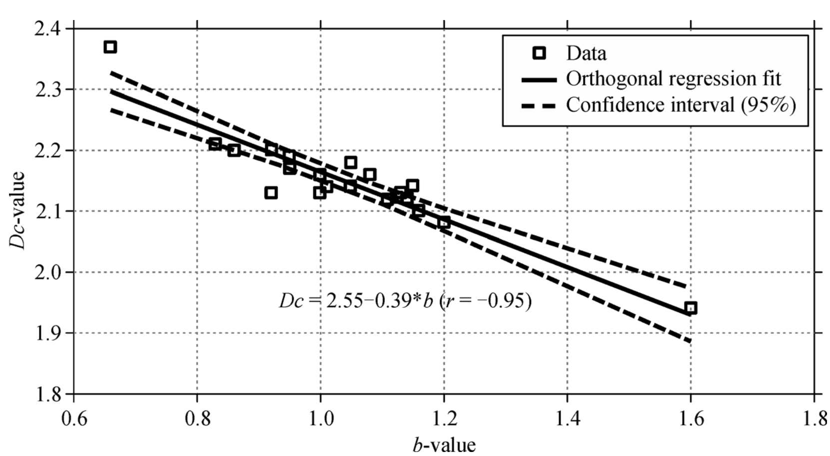

Fig. 9 Estimated orthogonal regression fit for the relationship between *b*-value and *Dc*-value. Resulting equation, correlation coefficient, and confidence interval of 95%, for the Eastern Anatolian Region of Turkey are also given. There are 12 events in the confidence interval of 95%.

temporal clustering, occurred between 1970 (M_D5.0) and 1985 (M_D5.0), 1991 (M_D4.8) and 1995 (M_D5.6), 1997 (M_D5.5), 1999 (M_D5.5), 2001 (M_D5.5), 2002 (M_D5.6), 2003 (M_D6.4), 2004 (M_D5.5), 2005 (M_D5.9), 2007 (M_D5.6), 2010 (M_D6.0), 2011 (M_D6.6), and 2012 (M_D5.5). Temporal changes in *Dc* and *b*-values against time are given in Fig. 11. Time distribution of correlation dimension is achieved to evaluate the possible temporal changes in Eastern Anatolia from 1970 to 2015. Because fewer earthquakes occurred between 1970 and 1996, annual calculations were not made. As shown in Fig. 11, *b*-values show a clear decrease in certain years, yet *Dc*-values

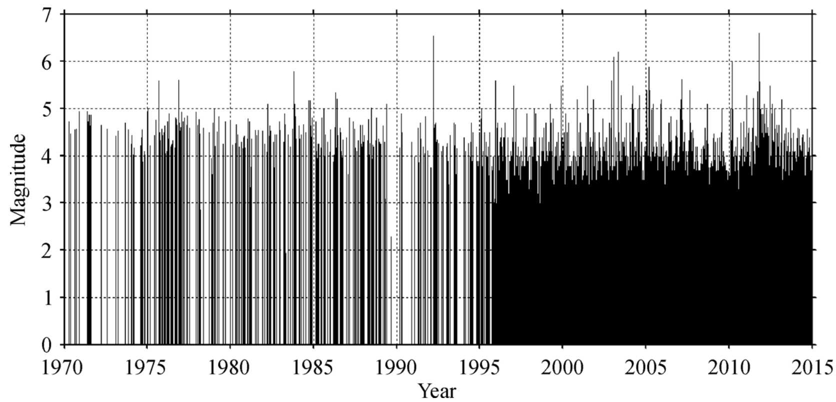

Fig. 10 Magnitude-time histogram for earthquake catalog of the Eastern Anatolian Region of Turkey between 1970 and 2015.

Table 2 Variations in the number of earthquakes, minimum (M_{min}) and maximum (M_{max}) magnitudes, *Mc*-values, *a*-value, *b*-value and *Dc*-value for the Eastern Anatolian Region of Turkey in time intervals between 1970 and 2015

Year	Earthquake Numbers	M_{min}	M_{max}	*Mc*-value	*a*-value	*b*-value	*Dc*-value
1970–1975	75	3.3	5.6	4.2	11.8	1.33±0.07	2.76±0.04
1976–1980	81	2.9	5.6	4.2	14.5	1.06±0.08	2.08±0.03
1981–1985	96	2.0	5.8	4.5	9.79	1.79±0.30	1.72±0.03
1986–1990	90	2.3	5.4	4.3	8.65	1.61±0.20	1.17±0.02
1991–1995	181	2.3	6.5	4.0	6.88	0.95±0.10	1.59±0.03
1996	143	2.4	4.7	3.5	5.49	1.02±0.09	2.11±0.03
1997	187	2.3	5.5	3.4	5.27	0.96±0.08	1.70±0.02
1998	155	2.6	5.0	3.2	4.71	1.15±0.08	2.07±0.02
1999	206	2.6	5.5	3.4	5.82	1.10±0.09	1.72±0.02
2000	305	2.4	5.2	3.0	5.02	1.19±0.07	2.60±0.02
2001	299	2.0	5.5	3.1	5.53	1.04±0.07	2.21±0.03
2002	409	2.2	5.6	3.1	6.11	1.19±0.07	2.02±0.03
2003	1427	2.3	6.2	3.0	7.22	1.49±0.04	2.82±0.06
2004	1350	2.3	5.5	3.0	6.91	1.31±0.04	2.58±0.04
2005	1489	2.4	5.9	3.0	6.45	1.16±0.04	2.58±0.05
2006	723	2.5	4.8	3.0	6.67	1.32±0.06	2.04±0.04
2007	1330	2.4	5.6	2.9	6.62	1.07±0.07	2.24±0.06
2008	1156	2.4	5.1	2.9	7.01	1.43±0.05	2.17±0.04
2009	1404	2.2	5.0	2.9	7.24	1.49±0.05	2.07±0.03
2010	2445	2.0	6.0	2.7	7.12	1.05±0.09	2.73±0.07
2011	6587	1.1	6.6	2.7	6.58	1.09±0.02	2.46±0.05
2012	6096	1.0	5.5	2.5	6.29	1.15±0.03	2.28±0.06
2013	4264	1.0	5.2	2.5	5.95	1.17±0.06	2.21±0.06
2014	3403	1.0	4.6	2.4	5.86	1.07±0.03	2.37±0.02

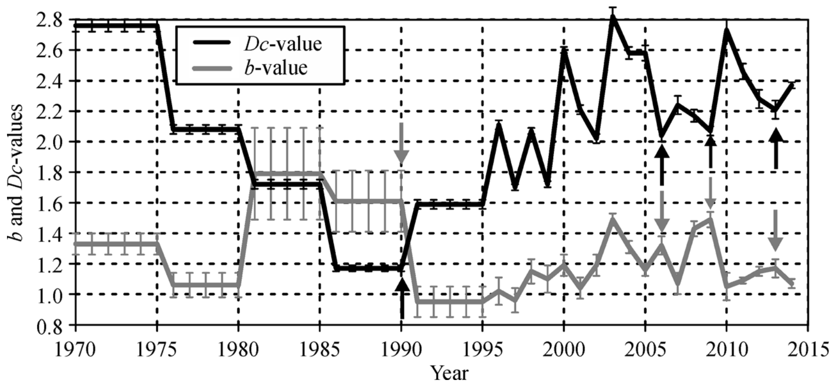

Fig. 11 Changes in two fundamental parameters *b* and *Dc*-values from 1970 to 2015 in the Eastern Anatolian Region of Turkey. Arrows show the starting times in decreasing *b*-values and increasing *Dc*-values. Standard errors are also shown.

show a clear increase in the same years. These anomalies are also clearly shown in Table 2 and by the arrows displayed in Fig. 11. For instance, *Dc*-value tends to increase, whereas the *b*-value tends to decrease, from 1990 to 1991. A stronger earthquake than that of 1990 occurred between 1991 and 1995. This same type of change is also observed between 2006 and 2007, 2009 and 2010, and 2013 and 2014. However, the same increase in magnitude is not observed from 2013 to 2014. Many factors can affect these parameters as stated above. In an active fault system, stress relaxation occurs on fault planes of smaller surface scale due to the relation between the lower *b*-values and the higher *Dc*-values. The higher order fractal dimension is increasingly sensitive to heterogeneity in the distribution of magnitudes. This suggests that seismicity is more clustered at larger scales (or in smaller areas) in Eastern Anatolia. These fluctuations in *b* and *Dc*-values can also be an indication of stress changes. Generally speaking, these changes mean this type of variation in *b* and *Dc*-values may be used for evaluating the next earthquake potential in this region of Turkey.

In the scope of this study, another aim is to investigate the seismic quiescence as a precursor at the beginning of 2015 in the Eastern Anatolian Region. To map the regional variation of the standard deviate *Z*-value, the study region is divided into a spatial grid of points with a distance of 0.05° in latitude and longitude. The nearest earthquakes, *N*, at each node are takes as 50 events. The changes in the seismic activity rate are then examined within a maximum radius which changes by a moving time window T_W (or i*wl*), stepping forward through a time series by a sampling interval as described by Wiemer and Wyss (1994). To maintain a continuous and dense coverage over time, the population of the earthquakes is binned into numerous 28 day spans for each grid point. T_W= 5.5 years is preferred as the window length due to the increased visibility of the quiescence areas for this time window. Each *Z*-value is represented by a different color: the scale spanning from the lowest *Z*-values, indicating no significant changes in seismicity rate, is shown in black; and the highest values indicating a decrease in seismicity rate, is shown in gray. The computed *Z*-values are then contoured and mapped.

Declustered data with $M_D \geqslant 2.9$ (10,468 events) was used to create the regional variations of the standard deviate *Z*-value at the beginning of 2015. Spatial distribution of *Z*-value with T_W= 5.5 years is mapped in Fig. 12. The length of T_W for the *Z*-value map was obtained by adding T_W-value to the time chosen as the beginning of the "cut at" time as indicated at the top of Fig. 12. Thus, *Z*-value changes are illustrated at the beginning of 2015. Six anomaly regions of seismic quiescence are shown in Fig. 12. These seismic quiescence regions are observed

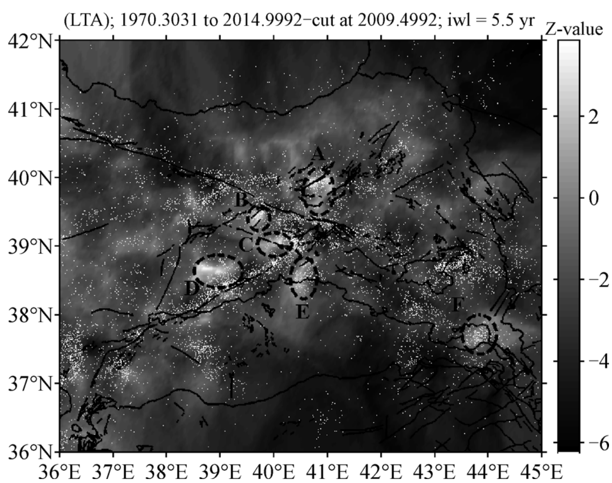

Fig. 12 Regional changes of standard deviate *Z*-value at the beginning of 2015 with T_W (*iwl*) equal to 5.5 years for the Eastern Anatolian Region of Turkey. White dots show the declustered events with $M_D \geqslant 2.9$. Significant quiescence anomalies detected at the beginning of 2015 are given as regions A (around NEAFZ, AKF and EZF), B and C (including PF and KKF), D (between MLF and EAFZ), E (around GF), and F (around YŞFZ). These regions with clear quiescence are important for estimating future seismic hazards and may show the locations of future earthquakes in the study region.

around the NEAFZ, Aşkale and Erzurum faults (region A), including Pülümür and Karakoçan faults (regions B and C), between the Malatya fault and EAFZ (region D), around the Genç fault (region E), and the Yüksekova-Şemdinli fault zone (region F). In addition to geographical distributions of *Z*-value for different T_W-values, regional variability of *Z*-values is shown in Fig. 13 and created annually from 2000 to 2015 by adding T_W= 5.5 years to the "cut at" times. In this presentation, the main goal is to map the temporal changes of spatial variation of *Z*-value. The quiescence anomalies detected in Fig. 12 are more visible for T_W= 5.5 years, as stated above, and thus, this length of this window is preferred for mapping the spatial variation of the seismicity rate changes in time. A decrease in seismicity is clearly observed in different time slices of Z-value between 2000 and 2015. Quiescence anomalies were observed for the "cut at" times between 2000 and 2003 (Figs. 13(a) – 13(d)) in the northern (in Black Sea), northeastern (including Caucasus), and southern areas (southeast parts of Turkey) of the study region. There is also a small quiescence area in the northeastern section of Lake Van in these time slices. However, seismic quiescence anomalies in the northern area of the study region were not observed at the "cut at" times of 2002 and 2003. Another anomaly is located in and around Lake Van for the time slices between 2004 and 2006 (Figs. 13(e) – 13 (g)). From the "cut at" time of 2007 (Fig. 13(h)), seismic quiescence regions associated with the beginning of 2015 began to appear in all areas of the study region. As seen in Figs. 13(h) – 13(j), there were no significant seismic quiescence anomalies until 2012.5 (cut at time is 2007) for the regions shown in Fig. 12. The significant occurrence of earthquakes, such as 2000 Van, 2003 Tunceli, 2003 Bingöl, 2004 Erzurum, 2005 Hakkari, 2004, 2010 Elazığ, and 2011 Van, indicates that seismic activity will continue. Seismic quiescence is not identified until this time period. However, these one-year maps show some clear quiescence regions after 2012, located approximately in the center of regions A, B, C, D, E, and F. As a result, the temporal variation of the spatial distribution of *Z*-value can be considered a successful tool for characterizing the beginning of quiescence.

As suggested in the studies of nonlinear time series analysis, these methods require data to be set up in a long data format at high quality. Kember and Fowler (1992) stated that following the reports of low dimensional dynamics in such complicated time series, the accurate estimation of attractor dimension requires exponentially long time series. They plotted the correlation integral using 1000 points and 5000 points, resulting in a more accurate result with the 5000 point calculation. However, as stated in Goltz (1998), the correlation dimension is more accurate for small data sets because it weighs heavier in those regions of embedded space that contain data (Grassberger and Procaccia, 1983). Also, *Dc* should be generally preferred if the expected fractal dimension is high (Smith, 1988). In addition, smaller data sets can be adequate if relative to the *Dc* values. As given in Table 1 and Table 2, the number of earthquakes for the calculation of *Dc*-values varies from 75 to 8847. These sample sizes seem to be sufficient for a relative estimation of correlation dimension. As a result, the well-known Grassberger and Procaccia correlation integral calculation algorithm is used to estimate fractal dimension because of its computational simplicity and most used for estimating the fractal dimension of processes with smaller data sets (Matcharashvili et al., 2000).

Matcharashvili et al. (2000) made a qualitative and quantitative evaluation of dynamical properties of Caucasian region earthquake time and size distributions. For this purpose, they achieved the nonlinear time series analysis of inter-event time intervals and magnitude sequences from the corresponding catalog using the Grassberger and Procaccia (1983) correlation integral calculation algorithm. They performed their analysis for time series of the whole Caucasus (11,683 events), the Greater Caucasus (3515 events), and the Javakheti Region (6694 events) from 1962 – 1993. Their results suggest the possibility of using non-statistical methods for prediction of earthquake time distribution, although further investigation is needed to reveal the precise nature of the low dimensional structure. However, their results do provide additional findings that the earthquake generation process neither random nor unpredictable in relation to space and time distribution domains. However, as stated in Matcharashvili et al. (2000), well-known scaling laws of earthquake time and size distributions have different underlying dynamics. The process cannot be identified as low dimensional chaos, and thus requires additional study. Consequently, in terms of possible forecasting of earthquake hazard potential, correlation dimension of earthquake distribution in the EAFZ is of significant importance as it is an efficient method for evaluating seismic risk and hazard.

Polat et al. (2008) achieved a seismic hazard analysis of the Aegean extension region of Turkey by using Gutenberg-Richter *b*-value, fractal dimension *Dc*-value, and seismic quiescence *Z*-value. Their analysis presents a significant hazard potential based on these types of size scaling parameters. They stated that the sites of greater *Z*-values and smaller *b*-values could be considered as the most probable areas for next events. Further evidence of these types of relations between Z and *b*-values are found in Öztürk and Bayrak (2012). These findings are also supported by findings that a decrease in *b*-value is related to an increase in stress release. In the present study, the lower *b*-values are observed in regions 4, 5, 9, 11, 12, and 18, whereas higher *Z*-values are observed in regions 2, 8, 11, 17, and 18. Given the combination of these parameters, regions 11 and 18, which cover Genç, Karakoçan, and Pülümür faults, should be considered as high risk for

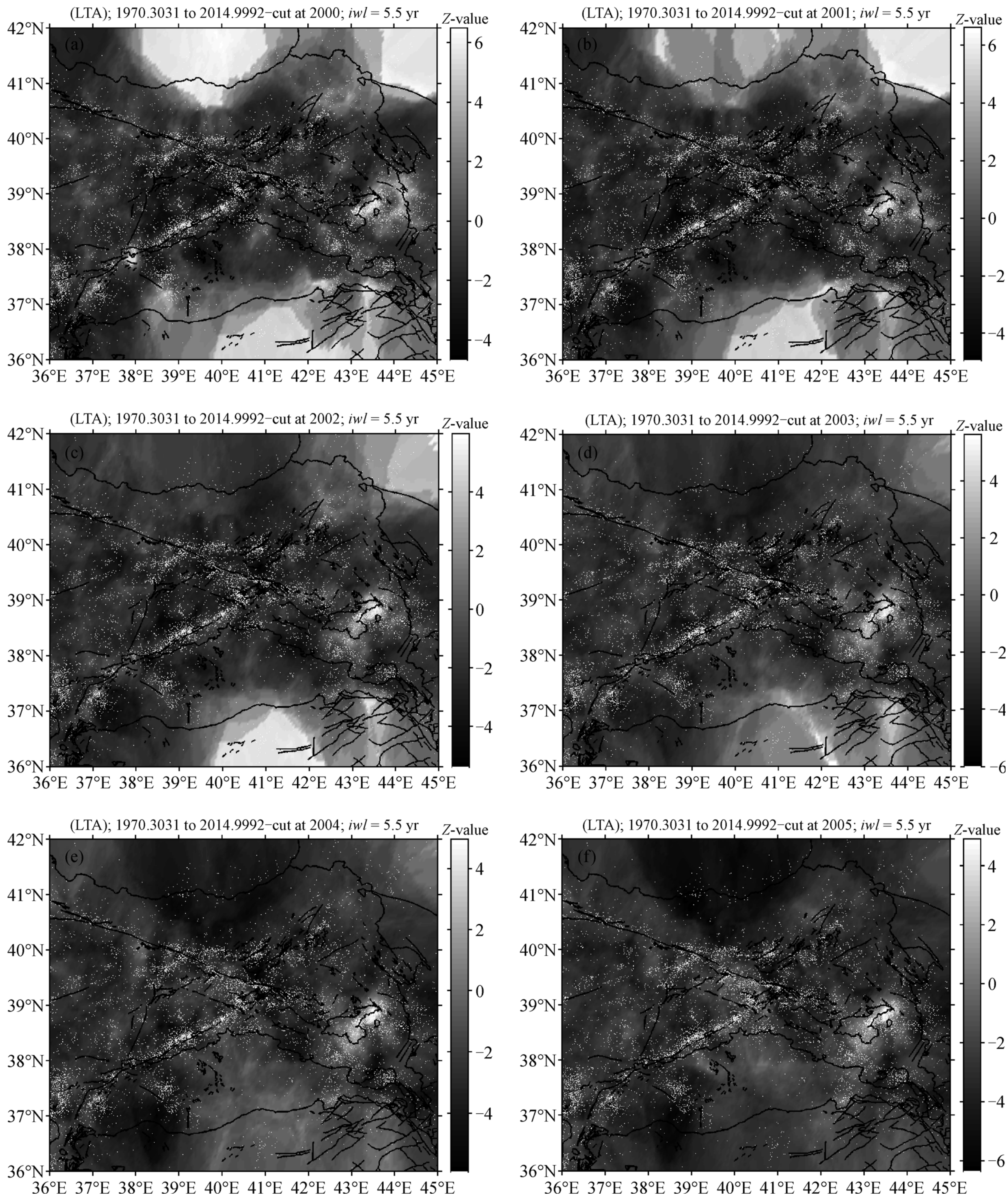
(LTA); 1970.3031 to 2014.9992−cut at 2000; iwl = 5.5 yr
Z-value
(a)
(LTA); 1970.3031 to 2014.9992−cut at 2001; iwl = 5.5 yr
Z-value
(b)
(LTA); 1970.3031 to 2014.9992−cut at 2002; iwl = 5.5 yr
Z-value
(c)
(LTA); 1970.3031 to 2014.9992−cut at 2003; iwl = 5.5 yr
Z-value
(d)
(LTA); 1970.3031 to 2014.9992−cut at 2004; iwl = 5.5 yr
Z-value
(e)
(LTA); 1970.3031 to 2014.9992−cut at 2005; iwl = 5.5 yr
Z-value
(f)
42°N 41°N 40°N 39°N 38°N 37°N 36°N
36°E 37°E 38°E 39°E 40°E 41°E 42°E 43°E 44°E 45°E
6 4 2 0 −2 −4 −6

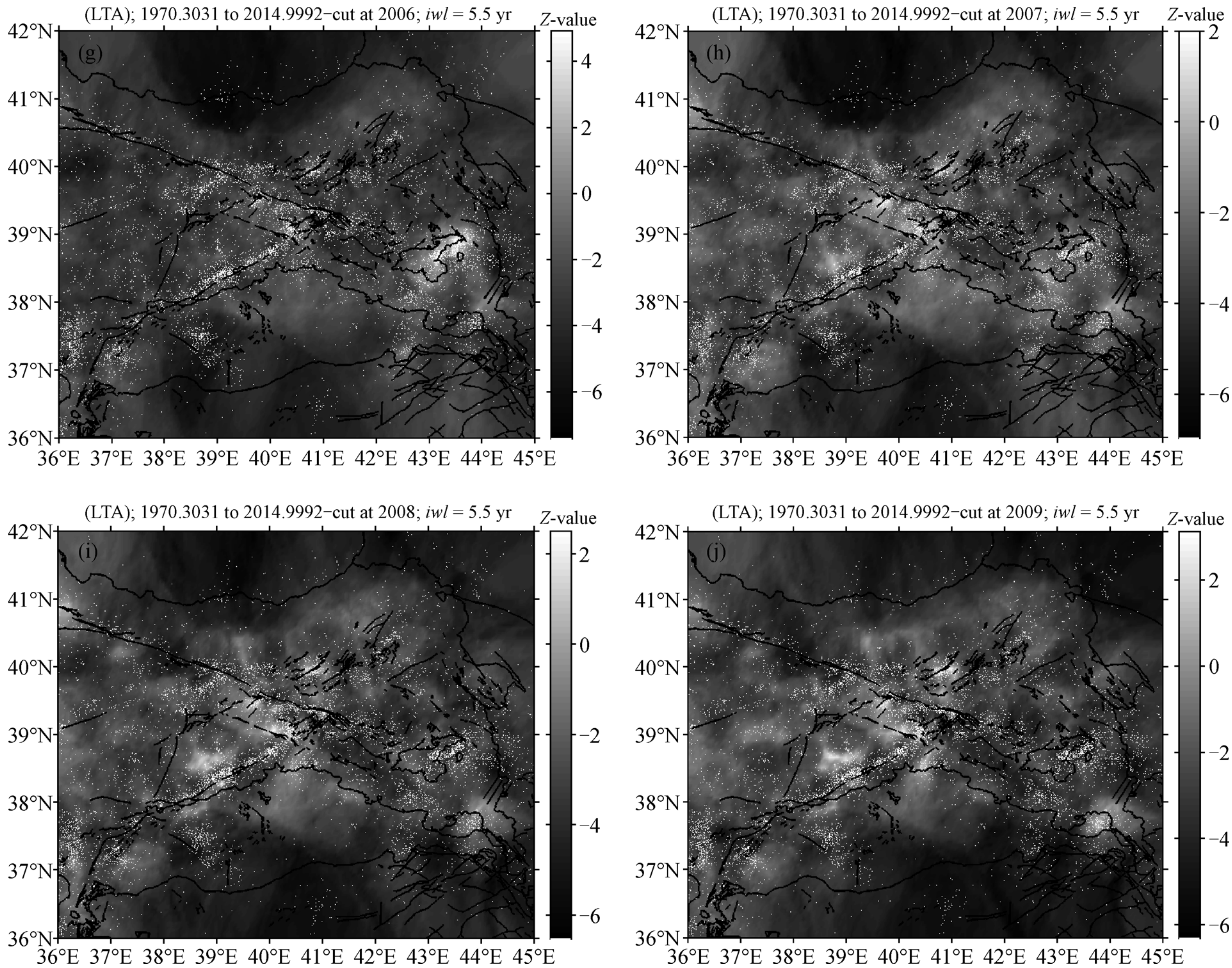

Fig. 13 Annual regional changes of standard deviate *Z*-value between 2000 and 2015 using the declustered events (white dots) with $M_D \geqslant 2.9$. T_W (*iwl*)= 5.5 years is selected as the length of time. Positive *Z*-value (gray color) represents the decrease in seismicity. "Cut at" times for *Z*-value distributions are considered for; (a) 2000, (b) 2001, (c) 2002, (d) 2003, (e) 2004, (f) 2005, (g) 2006, (h) 2007, (i) 2008, and (j) 2009.

potential earthquake occurrences.

Öztürk et al. (2008) evaluated earthquake hazards for different regions of Turkey using Gumbel's I method. They made a quantitative appraisal of parameters, such as the mean return period, the probable maximum magnitude, and the probability of a major earthquake occurrence for a given magnitude in different periods, such as 10, 25, 50, and 100 years in 24 different regions, including Region 1: the Northeast Anatolian Fault Zone, Region 2: Iğdır, Kağızman, Tutak, and Çaldıran faults, Region 3: Malazgirt, Erciş, and Süphan faults, and the Muş Thrust Zone, Region 4: Bitlis-Zagros Thrust Zone, Region 23: Ovacık and Malatya faults, and Region 24: covering the Eastern section of the North Anatolian Fault Zone, which are updated to provide a detailed comparison at a smaller scale. Öztürk et al. (2008) calculated the mean return period values for earthquakes with $Ms \geqslant 6.0$ in their regions of study per the following: their Region 1, covering the NEAFZ, AKF, EZF, and ÇFZ (Regions 1 and 2 in this study) is equal to 33.88±0.22 years; their Region 2, including IF, KF, AF, ÇF, BFZ, and DFZ (Regions 3 and 4 in this study), as 37.15±0.86 years; their Region 3, covering HTF, BF, ERF, MF, and SF (Regions 5, 6, and 7 in this study), as 104.71±7.29 years; their Region 4, including YŞFZ, KBF, BZTZ, GF, and MTZ (Regions 8, 9, 10, 11, and 12 in this study), as 34.67±3.97 years; their Region 7, consisting of the southwest section of EAFZ and the northern area of DSFZ (Regions 20 and 21 in this study), as 93.33±15.16 years; their Region 23, including PF, MLF, OF, and SRF (Regions 16 and 17 in this study), as 107.15±53.69 years; and their Region 24, including the eastern area of NAFZ, SUFZ, KKF, and GFZ (Regions 18 and 19 in this study), as 57.54±1.33 years. Considering the mean return periods for the earthquakes with magnitudes between 6.0 and 7.0 from Öztürk et al. (2008), the regions of NEAFZ, ÇFZ, IF, DFZ, ÇF, GF, PF, SUFZ, KKF, and GFZ have the highest potential for the next earthquake occurrence. Based on these results, the next major earthquake occurrence can be expected sometime in 2017.

Öztürk (2009) completed an earthquake hazard evaluation study in the Eastern section of Turkey by using standard deviate Z-value. He used several recent earthquakes larger than 5.0, during the time interval of 1970 and 2005 and estimated the duration of precursory seismic quiescence between 36°E and 45°E in longitude and 36°N and 42°N in latitude. He analyzed three earthquakes for the Van Region, two for the Tunceli Region, seven for the Bingöl Region, four for the Malatya Region, two for the Erzurum Region, and two for the Elazığ Region. Results from Öztürk (2009) show an average period of 5.0±1.5 years of precursory quiescence before the occurrence of a strong earthquake in this region. Considering the fact that observations of precursory quiescence began around 2012, and that the duration of seismic quiescence averages approximately five years, the next earthquake occurrence in the anomaly regions (regions A, B, C, D, E, and F in this study) can be expected in 2017. However, one can conclude that this prediction may extend into 2018 due to the standard deviation of seismic quiescence as ±1.5 years.

Öztürk and Bayrak (2012) made a statistical assessment for the eastern region of Turkey at the beginning of 2009 by considering the seismic quiescence phenomenon. Their analyses gave some interesting results, showing seismic quiescence and occurrence of two earthquakes in two of the four anomaly regions studied; one being the 2010 Elazığ earthquake and the other the 2011 Lake Van earthquake. In addition to the anomaly regions of Öztürk and Bayrak (2012), two new quiescence regions are observed in this study; one around YŞFZ (region 8) and the other between EAFZ and MLF (region 17). However, similar seismic quiescence was observed in and around AKF, EZF, PF, GF, and KKF. From this point of view, it is predicted that these anomaly regions, in which seismic quiescence was observed at the beginning of 2015, could experience a major earthquake in 2018. As a result, the data, and therefore the results for Z-values in the present work, are more up-to-date. Thus, these types of seismicity behaviors may be an important tool for forecasting the future earthquake occurrences.

Based on these observances, the regional and temporal evaluation of earthquake occurrences in recent years in Eastern Anatolia may be valuable evidence of future earthquake hazards. For this purpose, seismotectonic parameters, such as b and Dc-values, and seismic quiescence Z-value and their correlations, should be evaluated more sensitively to estimate the anomaly regions before the occurrence of any future major earthquake. Current seismic quiescence areas were observed at the beginning of 2015, with agreement of results for all parameters. The last earthquake "M_W = 5.5- Bingöl, 03 December 2015, at 01:27:06 UTC" occurred in one of the eastern regions of Turkey with a high hazard potential (around region C in Fig. 12). Due to the fact that the earthquake catalog and sub-regions are now more detailed and the anomaly regions have been updated, special interest should be given to the other anomaly regions.

6 Conclusions

A statistical assessment on the correlation between the Gutenberg-Richter b-value and the fractal dimension Dc-value has been made and the recent variations in seismic activity at the beginning of 2015 were evaluated by using the precursory seismic quiescence Z-value. For this purpose, this paper focuses on the regional and temporal properties of the earthquake distributions in the Eastern Anatolian Region of Turkey. Average completeness magnitude for this entire region, from 1970 to 2015, was calculated as 2.9. The region was divided into 21 different seismic source zones to make a detailed analysis. An increase in the seismicity was observed after 1996, and more importantly, fluctuations in the number of earthquakes with magnitudes greater than 5.5 were recorded after 2000. Hence, seismicity is more clustered at larger scales (or in smaller areas). There are clear fluctuations in temporal changes of b and Dc-values, and it thus can be assumed that future major earthquakes will occur. Because the lower b-values are related to the higher Dc-values, the North East Anatolian Fault Zone, Aşkale, Erzurum, Iğdır, and Çaldıran faults, Doğubeyazıt Fault Zone, around the Genç fault, the western area of the Bitlis-Zagros Thrust Zone, Pülümür and Karakoçan faults, and the Sancak-Uzunpınar Fault Zone having b-values smaller than 1.0 should be of significant interest. The orthogonal regression is also preferred in order to obtain a more up-to-date and reliable empirical relation between b and Dc-values. The relationship of $Dc = 2.55 - 0.39*b$ is estimated with a very strong negative correlation ($r = -0.95$) for the Eastern Anatolian earthquakes.

Spatial distribution of the seismicity rate changes, using the standard deviate Z-test generating LTA(t) function, was mapped with a moving time window T_W= 5.5 years, and the Z-value distribution at the beginning of 2015 was plotted. Six anomaly regions of seismic quiescence were observed: around the North East Anatolian Fault Zone, Aşkale and Erzurum faults, around the Yüksekova-Şemdinli Fault Zone, around Genç fault, including the Karakoçan and Pülümür faults, and between the Malatya and East Anatolian Fault Zone. However, the regions having lower b-values and higher Z-values cover the Genç, Karakoçan and Pülümür faults. As a significant result, the correlations between these seismotectonic parameters can supply significant evidence in order to evaluate the earthquake hazard potential in the Eastern Anatolian Region of Turkey.

Acknowledgements The author would like to thank Prof. Dr. Stefan Wiemer for providing *ZMAP* software and the anonymous reviewers for their useful and constructive suggestions to improve this paper. I am grateful to Prof. Dr. Dogan Kalafat (KOERI) for providing the earthquake catalog.

References

Aki K (1965). Maximum likelihood estimate of *b* in the formula log$N$ = $a-bM$ and its confidence limits. Bull Earthq Res Inst Univ Tokyo, 43: 237–239

Aki K (1981). A probabilistic synthesis of precursory phenomena. In: Simpson D W, Richards P G, eds. Earthquake Prediction: An International Review. Maurice Ewing Series. AGU, Washington, DC, 4: 566–574

Arabasz W J, Hill S J (1996). Applying Reasenberg's cluster analysis algorithm to regional earthquake catalogs outside California. Seismol Res Lett, 67(2): 30 (abstract)

Barton D J, Foulger G R, Henderson J R, Julian B R (1999). Frequency-magnitude statistics and spatial correlation dimensions of earthquakes at Long Valley Caldera, California. Geophys J Int, 138(2): 563–570

Bayrak Y, Öztürk S, Çınar H, Kalafat D, Tsapanos T M, Koravos G Ch, Leventakis G A (2009). Estimating earthquake hazard parameters from instrumental data for different regions in and around Turkey. Eng Geol, 105(3–4): 200–210

Bozkurt E (2001). Neotectonics of Turkey-a synthesis. Geodin Acta, 14 (1–3): 3–30

Carrol R J, Ruppert D (1996). The use and misuse of orthogonal regression estimation in linear errors-in-variables models. Am Stat, 50: 1–6

Chen C C, Wang W C, Chang Y F, Wu Y M, Lee Y H (2006). A correlation between the *b*-value and the fractal dimension from the aftershock sequence of the 1999 Chi-Chi, Taiwan, earthquake. Geophys J Int, 167(3): 1215–1219

Console R, Montuori C, Murru M (2000). Statistical assessment of seismicity patterns in Italy: are they precursors of subsequent events? J Seismol, 4(4): 435–449

Enescu B, Ito K (2002). Spatial analysis of the frequency-magnitude distribution and decay rate of aftershock activity of the 2000 Western Tottori earthquake. Earth Planets Space, 54(8): 847–859

Erdik M, Alpay B Y, Onur T, Sesetyan K, Birgoren G (1999). Assessment of earthquake hazard in Turkey and neighboring regions. Ann Geofis, 42: 1125–1138

Frohlich C, Davis S (1993). Teleseismic *b*-values: or, much ado about 1.0. J Geophys Res, 98(B1): 631–644

Goltz C (1998). Fractal and chaotic properties of earthquakes (Lecture Notes in Earth Sciences, 77). Springer-Verlag, 178 pp

Grassberger P, Procaccia I (1983). Measuring the strangeness of strange attractors. Physica, 9(D): 189–208

Gutenberg R, Richter C F (1944). Frequency of earthquakes in California. Bull Seismol Soc Am, 34: 185–188

Hempton M R (1987). Constraints on Arabian plate motion and extensional history of the Red Sea. Tectonics, 6(6): 687–705

Hirabayashi T, Ito K, Yoshii T (1992). Multifractal analysis of earthquakes. Pure Appl Geophys, 138(4): 591–610

Hirata T (1989a). Correlation between the *b*-value and the fractal dimension of earthquakes. J Geophys Res, 94(B6): 7507–7514

Hirata T (1989b). Fractal dimension of fault systems in Japan: fractal structure in rock fracture geometry at various scales. Pure Appl Geophys, 131(1–2): 157–170

Kagan Y Y (2007). Earthquake spatial distribution: the correlation dimension. Geophys J Int, 168(3): 1175–1194

Katsumata K, Kasahara M (1999). Precursory seismic quiescence before the 1994 Kurile Earthquake (Mw = 8.3) revealed by three independent seismic catalogs. Pure Appl Geophys, 155(2–4): 443–470

Kember G, Fowler A C (1992). Random sampling and the Grassberger-Procaccia algorithm. Phys Lett A, 161(5): 429–432

Mandelbrot B B (1982). The Fractal Geometry of Nature. San Francisco: Freeman Press

Matcharashvili T, Chelidze T, Javakhishvili Z (2000). Nonlinear analysis of magnitude and interevent time interval sequences for earthquakes of Caucasian region. Nonlinear Process Geophys, 7(1/2): 9–20

Mogi K (1967). Earthquakes and fractures. Tectonophysics, 5(1): 35–55

Mogi K (1969). Some features of recent seismic activity in and near Japan. 2. Activity before and after great earthquakes. Bull Earthq Res Inst Univ Tokyo, 47: 395–417

Mori J, Abercrombie R E (1997). Depth dependence of earthquake frequency-magnitude distribution in California: implications for the rupture initiation. J Geophys Res, 102(B7): 15081–15090

Öncel A O, Alptekin Ö, Main I G (1995). Temporal variations of the fractal properties of seismicity in the western part of the North Anatolian fault zone: possible artifacts due to improvements in station coverage. Nonlinear Process Geophys, 2(3/4): 147–157

Öncel A O, Main I G, Alptekin Ö, Cowie P A (1996). Temporal variations of the fractal properties of seismicity in the north Anatolian fault zone between 31°E and 41°E. Pure Appl Geophys, 146: 148–159

Öncel A O, Wilson T H (2002). Space-time correlations of seismotectonic parameters and examples from Japan and Turkey preceding the İzmit earthquake. Bull Seismol Soc Am, 92(1): 339–349

Öncel A O, Wilson T H (2004). Correlation of seismotectonic variables and GPS strain- measurements in western Turkey. J Geophys Res, 109(B11): B11306

Öncel A O, Wilson T H (2007). Anomalous seismicity preceding the 1999 Izmit event, NW Turkey. Geophys J Int, 169(1): 259–270

Ouillon G, Sornette D, Castaing C (1995). Organisation of joints and faults from 1-cm to 100-km scales revealed by optimized anisotropic wavelet coefficient method and multifractal analysis. Nonlinear Process Geophys, 2(3/4): 158–177

Öztürk S (2009). An application of the earthquake hazard and aftershock probability evaluation methods to Turkey earthquakes. Dissertation for PhD degree. Karadeniz Technical University, Trabzon, Turkey (in Turkish with English abstract)

Öztürk S (2011). Characteristics of seismic activity in the western, central and eastern parts of the North Anatolian Fault Zone, Turkey: temporal and spatial analysis. Acta Geophysica, 59(2): 209–238

Öztürk S (2012). Statistical correlation between *b*-value and fractal dimension regarding Turkish epicentre distribution. Earth Sciences Research Journal, 16(2): 103–108

Öztürk S (2013). A statistical assessment of current seismic quiescence along the North Anatolian Fault Zone: earthquake precursors.

Austrian Journal of Earth Sciences, 106(2): 4–17

Öztürk S (2015). A study on the correlations between seismotectonic *b*-value and *Dc*-value, and seismic quiescence Z-value in the Western Anatolian region of Turkey. Austrian Journal of Earth Sciences, 108 (2): 172–184

Öztürk S, Bayrak Y (2012). Spatial variations of precursory seismic quiescence observed in recent years in the eastern part of Turkey. Acta Geophysica, 60(1): 92–118

Öztürk S, Bayrak Y, Çınar H, Koravos G Ch, Tsapanos T M (2008). A quantitative appraisal of earthquake hazard parameters computed from Gumbel I method for different regions in and around Turkey. Nat Hazards, 47(3): 471–495

Polat O, Gok E, Yılmaz D (2008). Earthquake hazard of the Aegean Extension region (West Turkey). Turk J Earth Sci, 17: 593–614

Prasad S, Singh C (2015). Evolution of *b-values* before large earthquakes of $mb \geqslant 6.0$ in the Andaman region. Geol Acta, 13(3): 205–210

Reasenberg P A (1985). Second-order moment of Central California seismicity, 1969–1982. J Geophys Res, 90(B7): 5479–5495

Roy S, Ghosh U, Hazra S, Kayal J R (2011). Fractal dimension and *b*-value mapping in the Andaman-Sumatra subduction zone. Nat Hazards, 57(1): 27–37

Şaroğlu F, Emre O, Kuşcu O (1992). Active fault map of Turkey. General Directorate of Mineral Research and Exploration, Ankara, Turkey

Şengör A M C, Yılmaz Y (1981). Tethyan evolution of Turkey: a plate tectonic approach. Tectonophysics, 75: 181–241

Smith L A (1988). Intrinsic limits on dimension calculations. Phys Lett A, 133(6): 283–288

Teotia S S, Kumar D (2007). The Great Sumatra-Andaman earthquake of 26 December 2004 was predictable even from seismicity data of mb > 4.5: a lesson to learn from natüre. Indian J Mar Sci, 36(2): 122–127

Wiemer S (2001). A software package to analyze seismicity: ZMAP. Seismol Res Lett, 72(3): 373–382

Wiemer S, Katsumata K (1999). Spatial variability of seismicity parameters in aftershock zones. J Geophys Res, 104(B6): 13,135–13,151

Wiemer S, Wyss M (1994). Seismic quiescence before the Landers (M = 7.5) and Big Bear (6.5) 1992 earthquakes. Bull Seismol Soc Am, 84 (3): 900–916

Wiemer S, Wyss M (2000). Minimum magnitude of completeness in earthquake catalogs: examples from Alaska, the Western United States, and Japan. Bull Seismol Soc Am, 90(4): 859–869

Woessner J, Wiemer S (2005). Assessing the quality of earthquake catalogs: estimating the magnitude of completeness and its uncertainty. Bull Seismol Soc Am, 95(2): 684–698

Wu Y M, Chiao Y L (2006). Seismic quiescence before the 1999 Chi-Chi, Taiwan, M_W7.6 Earthquake. Bull Seismol Soc Am, 96(1): 321–327

Wyss M, Burford R O (1987). Occurrences of predicted earthquake on the San Andreas fault. Nature, 329(6137): 323–325

Wyss M, Klein F, Nagamine K, Wiemer S (2001). Anomalously high *b*-values in the south flank of Kilauea volcano: evidence for the distribution of magma below Kilauea’s East Rift Zone. J Volcanol Geotherm Res, 106(1 – 2): 23–37

Wyss M, Martirosyan A H (1998). Seismic quiescence before the M7, 1988, Spitak earthquake, Armenia. Geophys J Int, 134(2): 329–340

Wyss M, Sobolev G A, Clippard J D (2004). Seismic quiescence precursors to two M7 earthquakes on Sakhalin Island, measured by two methods. Earth Planets Space, 56(8): 725–740